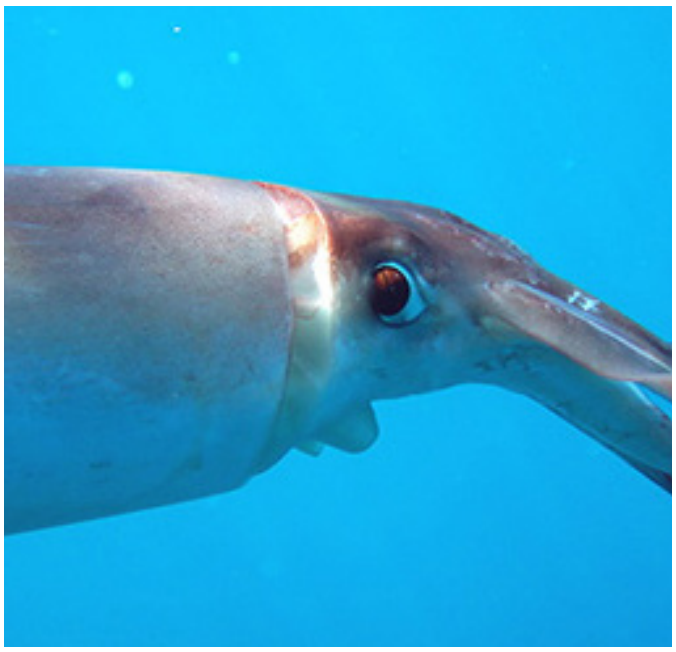

NOAA Scientific Publications Report

APRIL 12, 2013

HIGHLIGHTED ARTICLE

Quantifying climatological ranges and anomalies for coral reef ecosystems

Diarrhetic shellfish toxins and other polyether toxins of human health concern in Washington State

Osmotic stress does not trigger brevetoxin production in the dinoflagellate Karenia brevis

Extreme plasticity in life-history strategy allows a migratory predator (Dosidicus gigas) to cope with a changing climate

Oceans and marine resources in a changing climate

Effects of ocean acidification on hatch size and larval growth of walleye pollock (Theragra chalcogramma)

Quantifying climatological ranges and anomaly frequencies for Pacific Island reef ecosystems

Contents Continued...

ADDITIONAL ARTICLES

An integrated framework for informing coastal and marine ecosystem management decisions

Accounting for space-time interactions in index standardization models

Does reef fish catch saturate with increasing soak time or fish accumulation in a multispecies trap survey?

A springtime source of toxic Pseudo-nitzschia cells on Washington's razor clam beaches

Characterizing walleye pollock (Theragra chalcogramma) winter distribution from opportunistic acoustic data

Recovery of Acropora palmata in Curaçao: a comparison with the Florida Keys

Environments of Northeast U.S. severe thunderstorm events from 1999 to 2009

Early ontogeny of the mackerel icefish, Champsocephalus gunnari, in the southern Scotia Arc unities

A study on synoptic-scale tornado regimes

Circum-polar overview and spatial heterogeneity of Antarctic macrobenthic communities

A 1500-year reconstruction of annual mean temperature for temperate North America on decadal-to-multidecadal time scales

The distribution of the thermally tolerant symbiont lineage (Symbiodinium clade D) in corals from Hawaii: correlations with host and the history of ocean thermal stress

Impact of aeration and alkalinity on the water quality and product quality of transported tilapia - a simulation study

Comments on "An Objective High-Resolution Hail Climatology of the Contiguous United States"

UPLIGHTS: Upward Lightning Triggering Study

Long term monitoring of an endangered desert fish and factors influencing population dynamics

The Science of NOAA's Operational Hydrologic Ensemble Forecast Service

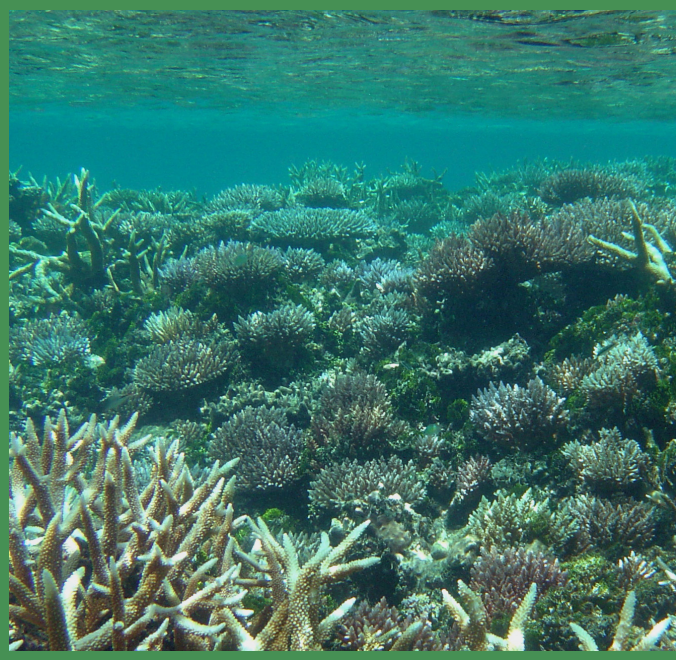

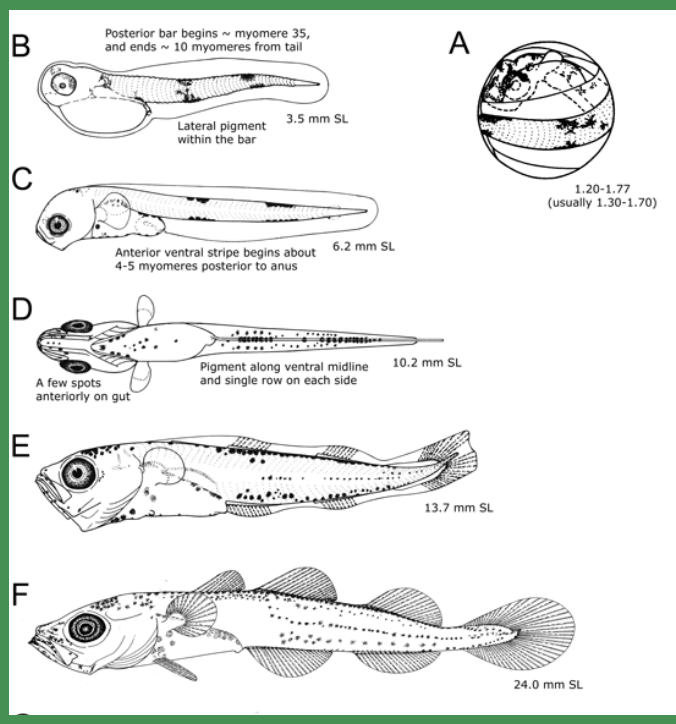

SALMON SUBSET

Genetic monitoring of threatened chinook salmon populations: estimating introgression of non-native hatchery stocks and temporal genetic changes

Effects of climate change on Oregon coast coho salmon: habitat and life-cycle interactions

Selective mortality on length, growth rate and rearing origin of juvenile chinook salmon (Oncorhynchus tshawytscha)

Using a stream network census of fish and habitat to assess models of juvenile salmonid distribution

OTHER REPORTS, BOOK CHAPTERS, & INTERNAL PUBLICATIONS

Dependence of IGS products on the ITRF datum

Towards the unification of the vertical datum over the North American continent

HIGHLIGHTED ARTICLE

AUTHORS

J. Gove (JIMAR/PIFSC), G. Williams, M. McManus, **S. Heron (James Cook University/NESDIS),** S. Sandin, **O. Vetter (JIMAR/PIFSC),** and **D. Foley (JIMAR/SWFSC)**

PUBLICATION DATE

Expected May 2013

TITLE

Quantifying climatological ranges and anomalies for coral reef ecosystems

JOURNAL

PLoS ONE

SIGNIFICANCE

- There is considerable spatial heterogeneity in climatological ranges across U.S. Pacific coral reef ecosystems.
- Assessing climatological conditions and historical anomalies may provide insight into coral reef ecosystem response to future climate scenarios.
- Although chlorophyll-a has been used as an indicator of stress-inducing environmental conditions on coral reefs, naturally elevated levels may positively influence coral reef ecosystems through increased food availability and/or enhanced levels of nutrients that are important for sessile benthic organisms such as corals and algae.

Healthy Coral Reef

SUMMARY

Coral reef ecosystems are exposed to a range of environmental forcings that vary on daily to decadal time scales and across spatial scales spanning from reefs to archipelagos. Environmental variability is a major determinant of coral reef ecosystem structure and function, including coral reef extent and growth rates, and the abundance, diversity and morphology of reef organisms. Proper characterization of environmental forcings on coral reef ecosystems is critical if we are to understand the dynamics and implications of abiotic–biotic interactions on reef ecosystems. This study combines high-resolution bathymetric information with remotely sensed sea surface temperature, chlorophyll-a and irradiance data, and modeled wave data to quantify environmental forcing on coral reefs. Results indicate considerable spatial heterogeneity in climatological ranges and anomalies across 41 islands and atolls, with emergent spatial patterns specific to each environmental forcing. For example, climatological wave energy was greatest at northern latitudes and generally decreased with latitude. In contrast, climatological chlorophyll-a was greatest at reef ecosystems proximate to the equator and northernmost locations, showing little synchrony with latitude. In addition, the authors find that reef ecosystems with the highest climatological chlorophyll-a concentrations are each uninhabited and are characterized by high hard coral cover and large numbers of predatory fishes. Finally, they find that uniquely scaling environmental data to the spatial footprint of individual islands and atolls is more likely to capture local environmental forcing, as chlorophyll-a concentrations decreased at relatively short distances (> 7 km) from 85% of the study locations. These metrics will help identify reef ecosystems most exposed to environmental stress and identify systems that may be more resistant and/or resilient to future climate change.

VISIT THE SCIENTIFIC PUBLICATIONS REPORT ARCHIVE

HIGHLIGHTED ARTICLE

AUTHORS

V. L. Trainer, L. Moore, B. D. Bill, N. G. Adams, N. Harrington, J. Borchert, **D. A. M. da Silva,** and B-**T. L. Eberhart (NMFS/NWFSC)**

PUBLICATION DATE

Expected April 2013

TITLE

Diarrhetic shellfish toxins and other polyether toxins of human health concern in Washington State

JOURNAL

Marine Drugs

SIGNIFICANCE

- Diarrhetic shellfish toxins are a new harmful algal bloom problem in Washington State which caused numerous closures in Puget Sound and the first ever closure on the WA Pacific coast in 2012.
- In 2011, three people from Washington State were the first ever in the US to become sick from diarrhetic shellfish poisoning.
- Volunteer phytoplankton monitoring provides an early warning of pending harmful algal blooms and assists the state with prioritizing shellfish sample analysis.

Toxic Shellfish Warning, Seattle, WA

SUMMARY

The illness of 3 people in 2011 after their ingestion of mussels collected from Sequim Bay State Park, Washington State, USA, demonstrated the necessity of monitoring diarrhetic shellfish toxins (DSTs) in Washington State for the protection of human health. Following these cases of diarrhetic shellfish poisoning, monitoring for DSTs in Washington State became formalized in 2012, guided by routine monitoring of *Dinophysis* spp. by the SoundToxins program in Puget Sound and the Olympic Region Harmful Algal Bloom (ORHAB) partnership on the outer Washington State coast. Here we show that the DSTs at concentrations above the guidance level of 16 µg okadaic acid (OA) + dinophysistoxins (DTXs) + pectenotoxins (PTXs)/100 g shellfish tissue were widespread in sentinel mussels throughout Puget Sound in summer 2012. Harvest closures of the California mussel, varnish clam, manila clam and Pacific oyster also occurred and included some recall of commercial product. Concentrations of toxins in Pacific oyster and manila clam were often at least half those measured in blue mussels at the same site. The primary toxin isomer in shellfish and plankton samples was dinophysistoxin-1 (DTX-1) with *D. acuminata* as the primary *Dinophysis* species. Other lipophilic toxins in shellfish were pectenotoxin-2 (PTX-2) and yessotoxin (YTX) with azaspiracid-2 (AZA-2) also measured in phytoplankton samples. Okadaic acid, azaspiracid-1 (AZA-1) and azaspiracid-3 (AZA-3) were all below the levels of detection by liquid chromatography tandem mass spectrometry (LC-MS/MS). A shellfish closure at Ruby Beach, Washington, was the first ever noted on the Washington State Pacific coast due to DSTs. The greater than average Fraser River flow during summer 2012 may have provided an environment conducive to dinoflagellates and played a role in the prevalence of toxigenic *Dinophysis* in Puget Sound.

VISIT THE SCIENTIFIC PUBLICATIONS REPORT ARCHIVE

HIGHLIGHTED ARTICLE

AUTHORS

W. G. Sunda, C. Burleson, **D. R. Hardison, J. S. Morey, Z. Wang,** J. Wolny, A. A. Corcoran, L. J. Flewelling, and **F. M. Van Dolah (NOS/NCCOS)**

PUBLICATION DATE

Expected April 2013

TITLE

Osmotic stress does not trigger brevetoxin production in the dinoflagellate Karenia brevis

JOURNAL

Proceedings of the National Academy of Sciences

SIGNIFICANCE

- Salinity changes within the normal range in coastal waters of the Gulf of Mexico (27 to 36) do not affect the growth rate of *K. brevis* cells and do not influence cell toxicity.
- This study contradicts a recently published article that a rapid decrease in salinity increased cellular toxin quotas in *K. brevis* and hypothesized that brevetoxins serve a role in osmoregulation.
- The authors suggest that the brevetoxins produced by *K. brevis* are more likely effective as chemical defences against grazers (e.g., zooplankton).

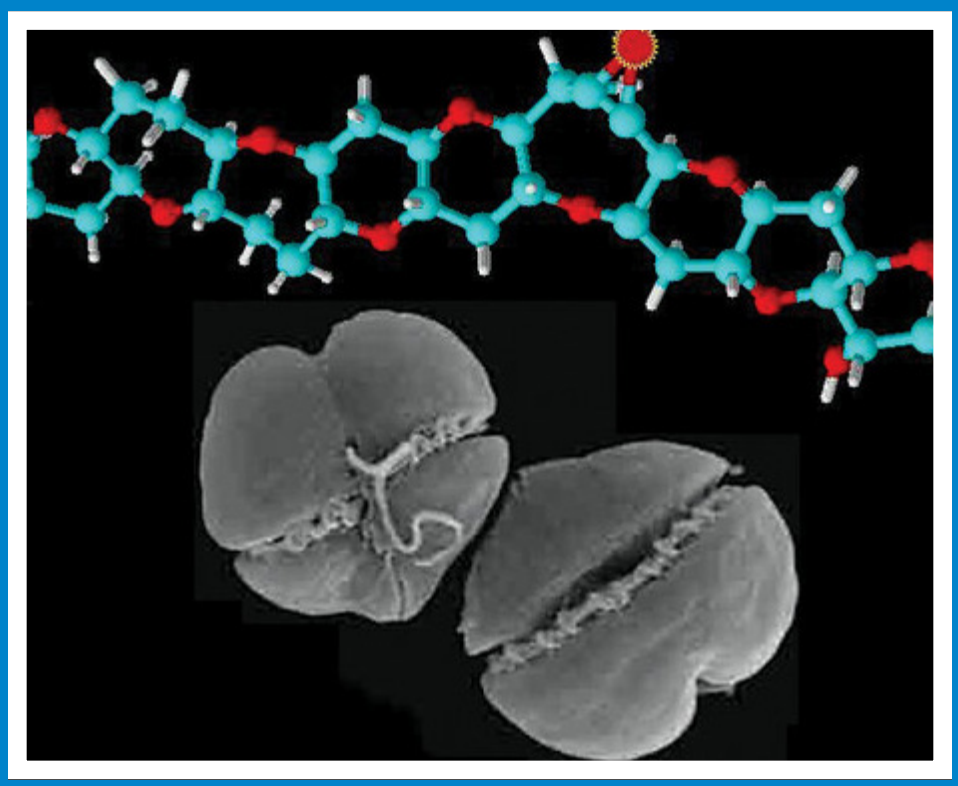

Brevetoxin & *Karenia Brevis*

SUMMARY

With the global proliferation of toxic harmful algal bloom (HAB) species, there is a need to identify the environmental and biological factors that regulate toxin production. One such species, *Karenia brevis,* forms nearly annual blooms that threaten coastal regions throughout the Gulf of Mexico. This dinoflagellate produces brevetoxins, potent neurotoxins that cause neurotoxic shellfish poisoning and respiratory illness in humans, as well as massive fish kills. A recent publication reported that a rapid decrease in salinity increased cellular toxin quotas in *K. brevis* and hypothesized that brevetoxins serve a role in osmoregulation. This finding implied that salinity shifts could significantly alter the toxic impacts of blooms. The authors repeated the original experiments separately in three different laboratories and found no evidence for increased brevetoxin production in response to low-salinity stress in any of the eight *K. brevis* strains we tested, including three used in the original study. Thus, they found no support for an osmoregulatory function of brevetoxins. The original publication also stated that there was no known cellular function for brevetoxins. However, there is increasing evidence that brevetoxins promote survival of the dinoflagellates by deterring grazing by zooplankton.

VISIT THE SCIENTIFIC PUBLICATIONS REPORT ARCHIVE

HIGHLIGHTED ARTICLE

AUTHORS

H.-J. Hoving, W. F. Gilly, U. Markaida, K. J. Benoit-Bird, Z. West-Brown, P. Daniel, **J. C. Field,** L. Parassenti, B. Liu, and B. Campos **(NMFS/SWFSC)**

PUBLICATION DATE

Expected Summer 2013

TITLE

Extreme plasticity in life-history strategy allows a migratory predator (Dosidicus gigas) *to cope with a changing climate*

JOURNAL

Global Change Biology

SIGNIFICANCE

- Jumbo squid are shown to have a high degree of life history plasticity (particularly size and age at maturity) in response to environmental forcing.
- This has great significance in the Gulf of California, where there is now a major fishery for this species, and may be related to the expansion and contraction of the population along the margins of their range (e.g., the California Current).

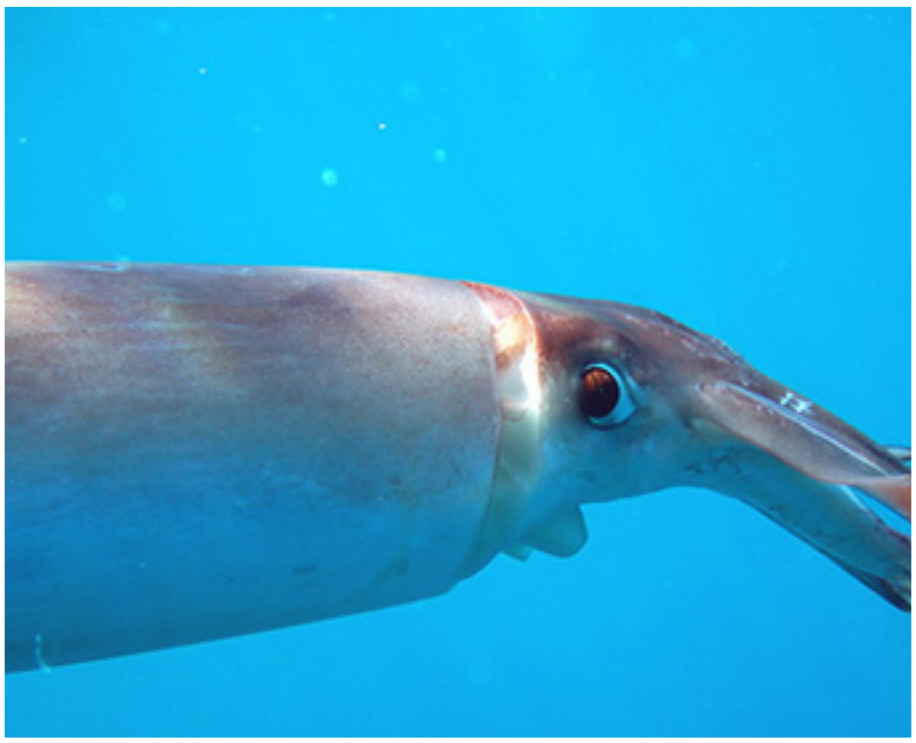

Dosidicus Gigas

SUMMARY

Dosidicus gigas (jumbo or Humboldt squid) is a semelparous, major predator of the eastern Pacific that is ecologically and commercially important. In the Gulf of California, these animals mature at large size (>55 cm mantle length) in 1-1.5 years and have supported a major commercial fishery in the Guaymas Basin during the last 20 years. An El Niño event in 2009-2010 was accompanied by a collapse of this fishery, and squid in the region showed major changes in distribution and life history strategy. Large squid abandoned seasonal coastal-shelf habitats in 2010 and instead were found in the Salsipuedes Basin to the north, an area buffered from the effects of El Niño by tidal upwelling and a well-mixed water column. The commercial fishery also relocated to this region. Although large squid were not found in the Guaymas Basin from 2010-2012, small squid were abundant and matured at an unusually small mantle-length (<30 cm) and young age (~6 months). Juvenile squid thus appeared to respond to El Niño with an alternative life-history trajectory in which gigantism and high fecundity in normally productive coastal-shelf habitats were traded for accelerated reproduction at small size in an offshore environment. Both small and large mature squid were present in the Salsipuedes Basin during 2011, indicating that both life history strategies can coexist. Hydro-acoustic data reveal that squid biomass in the study area nearly doubled between 2010 and 2011, primarily due to a large increase in small squid that were not susceptible to the fishery. Such a climate-driven switch in size-at-maturity may allow *D. gigas* to rapidly adapt to and cope with El Niño. This ability is likely to be an important factor in conjunction with longer-term climate-change and the potential ecological impacts of this invasive predator on marine ecosystems.

VISIT THE SCIENTIFIC PUBLICATIONS REPORT ARCHIVE

HIGHLIGHTED ARTICLE

AUTHORS

J. Howard (NMFS AAAS Fellow), E. a Babij, **R. Griffis (NMFS),** B. Helmuth, **A. Himes-Cornell (NMFS), P. Niemier (NMFS),** M. Orbach, **L. Petes (OAR),** S. Allen, G. Auad, **R. Beard (NESDIS),** M. Boatman, N. Bond, **T. Boyer (NESDIS), D. Brown (NESDIS), P. Clay (NMFS), K. Crane (OAR), S. Cross (NESDIS), M. Dalton (NMFS),** J. Diamond, R. Diaz, **Q. Dortch (NOS),** E. Duffy, **D. Fauquier (NMFS),** W. Fisher, M. Graham, B. Halpern, L. Hansen, B. Hayum, **S. Herrick (NMFS), A. Hollowed (NMFS),** D. Hutchins, **E. Jewett (OAR),** D. Jin, N. Knowlton, **D. Kotowicz (NMFS), T. Kristiansen (OAR),** P. Little, **C. Lopez (NOS),** P. Loring, **R. Lumpkin (OAR),** A. Mace, K. Mengerink , J. R. Morrison, J. Murray, **K. Norman (NMFS),** J. O'donnell, **J. Overland (OAR), R. Parsons (NESDIS),** N. Pettigrew, **L. Pfeiffer (NMFS),** E. Pidgeon, **M. Plummer (NMFS), J. Polovina (NMFS),** J. Quintrell, **T. Rowles (NMFS),** J. Runge, **M. Rust (NMFS),** E. Sanford, U. Send, M. Singer, **C. Speir (NMFS), D. Stanitski (OAR),** C. Thornber, **C. Wilson (NMFS),** and **Y. Xue (NWS)**

TITLE

Oceans and marine resources in a changing climate

PUBLICATION DATE

Expected June 2013

JOURNAL

Oceanography and Marine Biology Annual Review

SIGNIFICANCE

- This article is a synthesis of the current state of the knowledge surrounding climate impacts on marine systems and services.
- While no new scientific information is presented in the report, this is the only comprehensive review that spans the physical and biological changes to the ocean, social and economic impacts, and current international efforts.
- Projections of future change indicate that it is likely that marine ecosystems under U.S. jurisdiction, and U.S. activities and partnerships internationally, will continue to be affected by anthropogenic-driven climate change, and that those impacts will likely vary in magnitude and by region.

Oyster Harvest In Willapa Bay, Washington

SUMMARY

The United States is an ocean nation—our past, present, and future are inextricably connected to and dependent on oceans and marine resources. Marine ecosystems provide many important services, including jobs, food, transportation routes, recreational opportunities, health benefits, climate regulation, and cultural heritage that affect people, communities, and economies across the United States and internationally every day. There is a wealth of information documenting the strong linkages between the planet's climate and ocean systems, as well as how changes in the climate system can produce changes in the physical, chemical, and biological characteristics of ocean ecosystems on a variety of spatial and temporal scales. There is relatively little information on how these climate-driven changes in ocean ecosystems may have an impact on ocean services and uses, although it is predicted that ocean-dependent users, communities, and economies will likely become increasingly vulnerable in a changing climate. Based on our current understanding and future projections of the planet's ocean systems, it is likely that marine ecosystems will continue to be affected by anthropogenic-driven climate change into the future. This review describes how these impacts are set in motion through a suite of changes in ocean physical, chemical, and biological components and processes in U.S. waters, and the significant implications of these changes for ocean users and the communities and economies that depend on healthy oceans. U.S. international partnerships, management challenges, opportunities, and knowledge gaps are also discussed. Effectively preparing for and responding to climate-driven changes in the ocean will require both limiting future change through reductions of greenhouse gases and adapting to the changes that we can no longer avoid.

Please Note: This article is also being published in Island Press *as part of Technical Input Reports to the National Climate Assessment.*

VISIT THE SCIENTIFIC PUBLICATIONS REPORT ARCHIVE

HIGHLIGHTED ARTICLE

AUTHORS

T. P. Hurst (NMFS/AFSC), E. R. Fernandez, and **J. T. Mathis (OAR/PMEL)**

PUBLICATION DATE

Expected May 2013

TITLE

Effects of ocean acidification on hatch size and larval growth of walleye pollock (Theragra chalcogramma)

JOURNAL

ICES Journal of Marine Science

SIGNIFICANCE

This work found that that there was little effect of elevated levels of oceanic CO_2 on the sizes of newly hatched or early larval stages of walleye pollock.

The results may be taken out of context and are not meant to imply that this species (or any others) are completely immune to the effects of ocean acidification.

There are a range of other effects from ocean acidification which could negatively impact this species, but have yet to be explored.

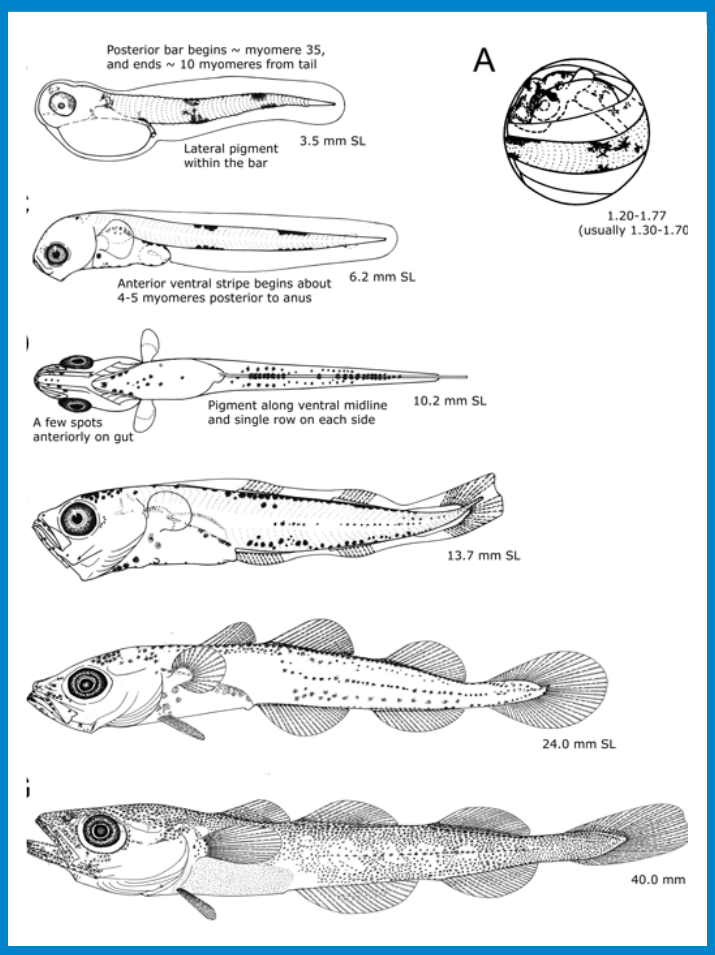

Walleye Pollock Developmental Stages

SUMMARY

Rising atmospheric concentrations of CO_2 are predicted to decrease the pH of high latitude oceans 0.3 to 0.5 units by 2100. Because of their limited capacity for ion-exchange, embryos and larvae of marine fishes are predicted to be more sensitive to elevated CO_2 than juveniles and adults. Eggs and larvae of walleye pollock (Theragra chalcogramma) were incubated across a broad range of CO_2 levels (280-2100 µatm) to evaluate sensitivity in this critical resource species. Slightly elevated CO_2 levels (~450 µatm) resulted in earlier hatching times, but differences among egg batches were greater than those observed across CO_2 treatments. Egg batches differed significantly in size-at-hatch metrics, but we observed no consistent effect of CO_2 level. In three independent experiments, walleye pollock were reared at ambient and elevated CO_2 levels through the early larval stage (to ~ 30 days post-hatch). Across trials, there were only minor effects of CO_2 level on size and growth rate, but fish in the ambient treatments tended to be slightly smaller than fish reared at elevated CO_2 levels. These results suggest that growth potential of early life stages of walleye pollock is resilient to the direct physiological effects of ocean acidification.

VISIT THE SCIENTIFIC PUBLICATIONS REPORT ARCHIVE

HIGHLIGHTED ARTICLE

AUTHORS

J. M. Gove (JIMAR/PIFSC), G. J. Williams, M. A. McManus, S. F. Heron, S. A. Sandin, **O. J. Vetter (JIMAR/PIFSC),** and **D. G. Foley (JIMAR/SWFSC)**

PUBLICATION DATE

Expected May 2013

TITLE

Quantifying climatological ranges and anomaly frequencies for Pacific Island reef ecosystems

JOURNAL

PLoS ONE

SIGNIFICANCE

- The results of this study aim to elucidate the differential importance of environmental forcings to coral reef communities across the U.S. Pacific coral reef ecosystems, fostering more targeted ecosystem research and aiding in the formulation of effective ecosystem-based management practices.
- This research will hopefully aid in the prediction of potential changes in coral reef ecology owing to a changing climate, an indisputable aspect of future reef system dynamics.

Pacific Island Reef Ecosystems

SUMMARY

Coral reef ecosystems are exposed to a range of environmental forcings that vary on daily to decadal time scales and across spatial scales spanning from reefs to archipelagos. Environmental variability is a major determinant of reef ecosystem structure and function, including coral reef extent and growth rates, and the abundance, diversity, and morphology of reef organisms. Proper characterization of environmental forcings on coral reef ecosystems is critical if we are to understand the dynamics and implications of abiotic–biotic interactions on reef ecosystems. This study combines high-resolution bathymetric information with remotely sensed sea surface temperature, chlorophyll-a and irradiance data, and modeled wave data to quantify environmental forcings on 9 coral reefs. We present a methodological approach to develop spatially constrained, island- and atoll-scale metrics that quantify climatological range limits and anomalous environmental forcings across U.S. Pacific coral reef ecosystems. Our results indicate considerable spatial heterogeneity in climatological ranges and anomalies across 41 islands and atolls, with emergent spatial patterns specific to each environmental forcing. For example, wave energy was greatest at northern latitudes and generally decreased with latitude. In contrast, chlorophyll-a was greatest at reef ecosystems proximate to the equator and northern-most locations, showing little synchrony with latitude. In addition, we find that the reef ecosystems with the highest chlorophyll-a concentrations; Jarvis, Howland, Baker, Palmyra and Kingman, are each uninhabited and are characterized by high hard coral cover and large numbers of predatory fishes. Finally, we find that scaling environmental data to the spatial footprint of individual islands and atolls is more likely to capture local environmental forcings, as chlorophyll-a concentrations decreased at relatively short distances (>7 km) from 85% of our study locations. These metrics will help identify reef ecosystems most exposed to environmental stress as well as systems that may be more resistant or resilient to future climate change.

VISIT THE SCIENTIFIC PUBLICATIONS REPORT ARCHIVE

ADDITIONAL ARTICLE

AUTHORS

M. Reiter, **G. Matlock (OAR/OPPE),** J. Gentile, M. Harwell, **R. Kelty (NOS/NCCOS), S. Baker (NOS/NCCOS), G. Scott (NOS/NCCOS),** and J. Barko

PUBLICATION DATE

Expected March 27, 2013

TITLE

An integrated framework for informing coastal and marine ecosystem management decisions

JOURNAL

Journal of Environmental Assessment Policy and Management

SIGNIFICANCE

- New tool available to evaluate complete ecosystem status and improve management decisions.
- The Integrated Assessment and Ecosystem Management Protocol (IAEMP) helps characterize potential causes of environmental problems, select appropriate response options, and implement and evaluate the selected option, thereby either addressing the concern or improving the ecosystem model for future decisions.

SUMMARY

Ecosystem management requires understanding society's goals for an ecosystem and managing for some optimal solution. Unlike terrestrial ecosystem managers, coastal and marine ecosystem management seldom integrates across sectors or scientific disciplines to achieve desired social benefits. An Integrated Ecosystem Assessment (IEA) considers the ecosystem (including humans) as a unit and can assist in setting goals, determining an ecosystem's ability to support ecological processes and society's desires, and predicting the outcome of alternatives. The use of Coupled Ecological-Societal Systems Models utilized within the Integrated Assessment and Ecosystem Management Protocol (IAEMP) allows managers to extend a graphical picture of risk analysis hypotheses to forecast scenarios that can be analyzed relative to management goals. Scenarios predicted to meet management goals are evaluated against management constraints to select the "optimal" option for a management action in an adaptive management process. The IAEMP thus helps characterize potential causes of environmental problems, select appropriate response options, and implement and evaluate the selected option, thereby either addressing the concern or improving the ecosystem model for future decisions.

LINK

http://www.worldscientific.com/doi/abs/10.1142/S1464333213500038

ADDITIONAL ARTICLE

AUTHORS

J. T. Thorson and **E. J. Ward (NMFS/NWFSC)**

PUBLICATION DATE

Expected Summer 2013

TITLE

Accounting for space-time interactions in index standardization models

JOURNAL

Fisheries Research

SIGNIFICANCE

- Models used to estimated indices of abundance from fish survey data can account for spatial variation changing over time.
- A positive relationship between occurrence probability and density is supported for several West Coast groundfishes.
- Different treatments of spatial variation changing over time have little effect on resulting estimates of abundance.
- The random effect models developed in this paper can now be quickly evaluated for species throughout the U.S. and the software is freely available and will be used to estimate abundance indices for U.S. West Coast species starting in 2013 assessments

SUMMARY

Scientific survey data are used to estimate abundance trends for fish populations worldwide, and are frequently analyzed using delta-generalized linear mixed models (delta-GLMMs). Delta-GLMMs incorporate information about both the probability of catch being non-zero (catch probability) and the expected value for non-zero catches (catch rates). Delta-GLMMs generally incorporate year as a main effect, and frequently account for spatial strata and/or covariates. Many existing delta-GLMMs do not account for random or systematic differences in catch probability or rates in particular combinations of spatial strata and year (i.e. space-time interactions), and do not recognize potential correlation in random space-time interactions between catch probability and catch rates. The authors therefore developed a Bayesian delta-GLMM that estimates correlations between catch probability and rates, and compare it with either (a) ignoring year-strata interactions, (b) modeling year-strata interactions as fixed effects, or (c) estimating year-strata interactions in catch probability or rates as independent random effects. These four models are fitted to bottom trawl survey data for 28 species off the U.S. West Coast. The posterior median of the correlation is positive for the majority (18) of species, including all five for which the posterior distribution has little overlap with zero. However, estimating this correlation has little impact on resulting abundance indices or credible intervals. The authors conclude that the correlated random model will have a little impact on index standardization of the West Coast bottom trawl dataset. However, they propose that the correlated model can quickly identify correlations between occupancy probability and density, and allow researchers to quickly identify whether such a correlation is likely to be significantly different from zero for their chosen data set.

VISIT THE SCIENTIFIC PUBLICATIONS REPORT ARCHIVE

ADDITIONAL ARTICLE

AUTHORS

N. M. Bacheler (NMFS/SWFSC), V. Bartolino, and M. J. M. Reichert

PUBLICATION DATE

Expected Late 2013

TITLE

Does reef fish catch saturate with increasing soak time or fish accumulation in a multispecies trap survey?

JOURNAL

Fishery Bulletin

SIGNIFICANCE

- Evidence that catch, not CPUE, should be used as the response variable in models indexing abundance in a standardized way.
- Soak time and number of total individuals caught in the trap should be included as predictor variables in the models.
- Researchers must consider the fact that catch of fish in traps likely saturates relatively quickly, so determining whether catch at saturation indexes true abundance linearly is an extremely important future research question.

SUMMARY

Catch rates from fishery-independent surveys are often assumed to vary in proportion to the actual abundance of the population, but this approach assumes that the catchability coefficient (q) is constant. When the rate at which gear catches fish declines as fish accumulate in the gear, catch saturates and q declines with longer fishing times. The authors used long-term trap survey data from the southeastern U.S. Atlantic to determine whether catches of eight reef fish species saturated due to the amount of time traps soaked or the level of fish accumulation (the total number of all species caught in the trap). They utilized a delta-model to relate the catch of each species to a variety of predictor variables to determine how catch was influenced by soak time and fish accumulation after accounting for variability in catch due to the other predictor variables in the model. They found evidence of saturation for all eight reef fish species examined. Most species had catches that saturated across the range of soak times examined, but three species had catches that saturated due to the fish accumulation levels in the trap. To infer relative abundance levels from catch data, their results suggest that future studies should standardize catch or catch rates using nonlinear regression models that incorporate soak time, fish accumulation, and any other predictor variable that may ultimately influence catch. Determining the exact mechanisms that cause fish to saturate fishing gears is a critical need, and their results suggest that these mechanisms may vary considerably among species.

VISIT THE SCIENTIFIC PUBLICATIONS REPORT ARCHIVE

ADDITIONAL ARTICLE

AUTHORS

B. M. Hickey, **V. L. Trainer,** P. M. Kosro, **N. G. Adams,** T. P. Connolly, N. B. Kachel, and S. L. Geier **(NMFS/NWFSC)**

PUBLICATION DATE

Expected April 2013

TITLE

A springtime source of toxic Pseudo-nitzschia *cells on Washington's razor clam beaches*

JOURNAL

Harmful Algae

SIGNIFICANCE

- Sources of domoic acid to the Washington State razor clam beaches are physically retentive sites, Heceta Bank (off central Oregon) and Juan de Fuca eddy (at the US/Canadian border).
- Heceta Bank is a springtime source of toxic harmful algal blooms to the WA coast, while the Juan de Fuca eddy is a source for summer and early fall blooms.
- The Columbia River can facilitate the rapid transport of cells from off the Oregon coast to WA beaches.
- This information will assist with ecological forecasting and will provide an early warning of harmful algal blooms in the Pacific Northwest which can cause >$22 million in lost revenue annually to the WA coastal region.

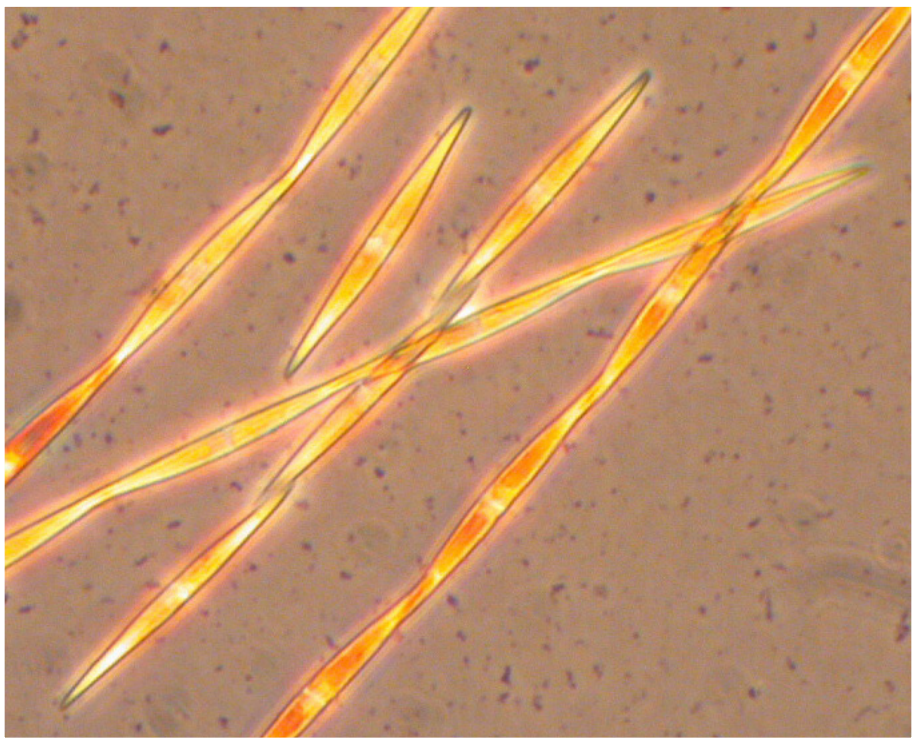

Pseudo-nitzschia Cells

SUMMARY

Concentrations of domoic acid (DA) above the regulatory limit in Washington coast razor clams are more common on northern beaches from summer to fall. Recent field studies have confirmed that the primary site of *Pseudo-nitzschia* (PN), a genus that contains several species of diatoms known to produce the neurotoxin DA, in those seasons is a semi-retentive topographically-trapped seasonal eddy located offshore and north of the clamming beaches. Another semi-retentive coastal feature, Heceta Bank, that has been shown to support toxic PN cells in the summer, is located south of Washington's clamming beaches. The authors present evidence that Heceta Bank, although not a likely source of toxic cells in summer due to the prevailing southward seasonal currents, may be a source of cells in springtime before those currents develop. The likelihood of Heceta Bank being a springtime southern source of DA is explored using biological and transport data surrounding a period of toxic razor clams in April 2005. In particular, satellite-derived chlorophyll data confirm that a bloom occurred over Heceta Bank in March of that year, just prior to a period of strong storm-driven northward transport. PN cells were observed during the April bloom on Washington's beaches and were documented in offshore Oregon waters on the northern edge of Heceta Bank. The PN species P. australis, has been shown to be highly toxic in this region and shore-based data show that Oregon razor clams were also toxic at the time when P. australis was observed offshore. Both measured and modeled currents show that transport is more than sufficient to move cells from the vicinity of Heceta Bank, Oregon to southern Washington beaches and the rapid transport is likely due, in part, to the presence of the buoyant plume from Columbia River, a common feature in winter and spring in nearshore waters of the U.S. Pacific Northwest.

LINK

http://www.sciencedirect.com/science/article/pii/S1568988313000206

VISIT THE SCIENTIFIC PUBLICATIONS REPORT ARCHIVE

ADDITIONAL ARTICLE

AUTHORS

S. J. Barbeaux, J. Horne, and **M. Dorn (NMFS/AFSC)**

PUBLICATION DATE

Expected April 20, 2013

TITLE

Characterizing walleye pollock (Theragra chalcogramma) *winter distribution from opportunistic acoustic data*

JOURNAL

ICES Journal of Marine Science

SIGNIFICANCE

- Acoustic data collected opportunistically from commercial fishing vessels are useful in describing the spatial and temporal distribution of fished aggregations, more so than other fishery dependent data sources.
- The pattern of pollock distribution is scale dependent and analyses should consider spatial and temporal resolutions.
- Pollock aggregations demonstrate a diel pattern expanding at night and contracting during the day both horizontally and vertically.

Walleye Pollock

SUMMARY

In 2003, acoustic data from 25,000 km of ship track lines were collected from two fishing vessels participating in the eastern Bering Sea walleye pollock *(Theragra chalcogramma)* fishery. Although these data were not calibrated or collected on a systematic grid, their broad temporal extent combined with high spatial resolution facilitated examination of the distribution and behaviour of fished aggregations. To demonstrate their scientific applicability, these data were used to identify spatio-temporal dynamics of pollock aggregations over scales ranging from hundreds of meters to hundreds of kilometres and from minutes to months. The spatial analysis identified three levels of pollock aggregation. The largest regions of high pollock density had an average diameter of 110 km and were comparable to distinct fishing grounds identified by fishers. The next smaller areas of high pollock density had a diameter between 2.5 and 6 km. Within these areas were clusters of pollock at even higher densities. The extent of the smallest aggregations ranged in diameter from 0.1 km in daylight to 0.6 km at night. Time series analysis identified vertical and horizontal diel changes in pollock distribution and an overall decline in pollock density over the study period.

VISIT THE SCIENTIFIC PUBLICATIONS REPORT ARCHIVE

ADDITIONAL ARTICLE

AUTHORS

A. J. Bright, D. E. Williams, K. L. Kramer, and **M. W. Miller (NMFS/SEFSC and CIMAS)**

PUBLICATION DATE

Expected 2013

TITLE

Recovery of Acropora palmata *in Curaçao: a comparison with the Florida Keys*

JOURNAL

Bulletin of Marine Science

SIGNIFICANCE

- The well-studied, genotypically depauperate elkhorn coral populations in the Florida Keys appear at least as resilient (at least to hurricane disturbance) as those diverse populations in Curaçao that were hypothesized to be more resilient.
- This provides important insights on the relationship of genotypic diversity and resilience in this ESA listed (proposed to be uplisted) coral.

Acropora palmata (Elkhorn Coral)

SUMMARY

Demographic monitoring of fixed plots of *Acropora palmata* in Curaçao and the Florida Keys before and after acute tropical storm disturbance allowed for a comparison of recovery processes. The Curaçao population was characterized by greater colony size, live tissue abundance and genotypic richness than the Florida Keys population, and hence was hypothesized to display a faster rate of recovery. However, after each population lost approximately half of its live tissue as a result of disturbance, magnitude of recovery differed significantly between regions. Despite high post-disturbance asexual recruitment of fragments in Curaçao (12.1 ± 4.9 recruits/plot compared to 4.6 ± 1.5 for Florida Keys), consistent with the original hypothesis, Curaçao populations have shown negligible recovery in terms of live tissue abundance (-2%) and have declined in number of colonies, whereas the Florida Keys population has shown a slight, significant increase in live tissue (13%) over the surveyed recovery period (from seven to 31 months post-disturbance).

VISIT THE SCIENTIFIC PUBLICATIONS REPORT ARCHIVE

ADDITIONAL ARTICLE

AUTHORS

M. M. Hurlburt, and **A. E. Cohen (NWS/NCEP/SPC)**

PUBLICATION DATE

Expected May 2013

TITLE

Environments of Northeast U.S. severe thunderstorm events from 1999 to 2009

JOURNAL

Weather and Forecasting

SIGNIFICANCE

- Meteorological summer months and peak diurnal heating favor complexes of thunderstorms that will produce a greater number of severe weather reports.
- Steep low-mid level lapse rates, as well as mixed layer convective inhibition and downdraft convective available potential energy are parameters that distinguish between events that produce few reports compared to those that produce a greater number of reports.
- The location of the upper trough and its attendant zones of strongest deep layer winds relative to the Northeast can be a predictor in the number of reports that will occur.

SUMMARY

An investigation of the environments and climatology of severe thunderstorms from 1999 through 2009 across the northeastern United States is presented. A total of 742 severe weather events producing over 12,000 reports were examined. Given the challenges that severe weather forecasting can present in the Northeast, this study is an effort to distinguish between the more prolific severe-weather-producing events and those that produce only isolated severe weather. The meteorological summer months (June, July, and August) are found to coincide with the peak severe season. During this time, 850-500-hPa and 700-500-hPa lapse rates, mixed layer convective inhibition (MLCIN) and downdraft convective available potential energy (DCAPE) are found to be statistically significant in discriminating events with a large number of reports from those producing fewer reports, based on observed soundings. Composite synoptic pattern analyses are also presented to spatially characterize the distribution of key meteorological variables associated with severe weather events of differing magnitudes. The presence of a mid-level trough and particular characteristics of its tilt, along with an accompanying zone of enhanced flow, are found in association with the higher-report severe weather events, along with cooler mid-level temperatures overlaying warmer low-level temperatures (i.e., contributing to the steeper lapse rates). During the meteorological fall and winter months (September through February), large-scale ascent is often bolstered by the presence of a coupled upper-level jet structure.

VISIT THE SCIENTIFIC PUBLICATIONS REPORT ARCHIVE

ADDITIONAL ARTICLE

AUTHORS

M. La Mesa, B. Catalano, P. Koubbi, and **C. D. Jones (NMFS)**

PUBLICATION DATE

Expected April 2013

TITLE

Early ontogeny of the mackerel icefish, Champsocephalus gunnari, *in the southern Scotia Arc unities*

JOURNAL

Polar Biology

SIGNIFICANCE

- Through the analysis of sagittal otoliths microstructure, we assessed the timing and duration of egg incubation, larval hatching, first exogenous feeding, rate of yolk resorption and body growth rate.
- Newly hatched larvae of Mackerel ice fishes exhibit a considerable amount of yolk supply, enabling them to postpone the starting of exogenous feeding in the event of an unforeseen decrease in prey availability.
- The capability of exogenous feeding during early ontogeny could result in the delayed yolk resorption and mixed feeding we observed in this study.

SUMMARY

During the early ontogeny of fishes, the timing and duration of key events such as larval hatching and the switch from endogenous to exogenous feeding largely determine the offspring viability and survival. The aim of the present study was to investigate the life history traits of the early larvae of the mackerel icefish, C*hamps-ocephalus gunnari,* collected in summer south of the South Shetland Islands in the Bransfield Strait and north of Elephant Island. Through the analysis of sagittal otolith microstructure, we assessed the timing and duration of egg incubation, larval hatching, first exogenous feeding, rate of yolk resorption and body growth rate. Compared to populations living further north (i.e. around South Georgia and Kerguelen Islands), mackerel icefish in the southern Scotia Arc exhibits longer egg incubation (lasting 90–120 days from winter to summer) and delayed hatching time spread over a relatively short period lasting 26 days between January and February. The first exogenous feeding takes place between 13 and 24 days after hatching still in the presence of the yolk-sac, indicating a prolonged mixed feeding afterward. The specific growth rate or daily percentage change in size (G) was 1.9 % SL day-1, corresponding to a daily growth rate at mean size of 0.31 mm day-1. While showing significant differences in early life history traits across their geographical distribution, *C. gunnari* populations share a common strategy, spawning a small number of large eggs that hatch in relatively large sized larvae, at a time which may be independent of the timing of pack-ice retreat and onset of the production cycle.

VISIT THE SCIENTIFIC PUBLICATIONS REPORT ARCHIVE

ADDITIONAL ARTICLE

AUTHORS

J. M. Garner (NWS/NCEP)

PUBLICATION DATE

Expected Spring/early summer 2013

TITLE

A study on synoptic-scale tornado regimes

JOURNAL

Journal of Severe Storms Meteorology

SIGNIFICANCE

- The magnitude of shear and buoyancy favorable for tornadic supercells is different for cold fronts, warm fronts, and drylines.
- This research provides guidance to operational forecasters responsible for anticipating tornado environments.

SUMMARY

The significant tornado parameter (STP) has been used by severe thunderstorm forecasters since 2003 to identify environments that are favorable for the development of strong to violent tornadoes. The STP and its individual components of mixed-layer (ML) CAPE, 0–6-km bulk wind difference (BWD), 0–1-km storm-relative helicity (SRH), and ML lifted condensation level (LCL) have been calculated here using archived surface objective analysis data, and then examined during the period 2003–2010 over the central and eastern United States. These components then were compared and contrasted in order to distinguish between environmental characteristics analyzed for three different synoptic-cyclone regimes that produced significantly tornadic supercells: cold fronts, warm fronts, and drylines. Results show that MLCAPE contributes strongly to the dryline significant-tornado environment, while it was less pronounced in cold-frontal significant-tornado regimes. The 0–6-km BWD was found to contribute equally to all three significant tornado regimes, while 0–1-km SRH more strongly contributed to the cold-frontal significant-tornado environment than for the warm-frontal and dryline regime.

VISIT THE SCIENTIFIC PUBLICATIONS REPORT ARCHIVE

ADDITIONAL ARTICLE

AUTHORS

J. Gutt, H. J. Griffiths, and **C. D. Jones (NMFS)**

PUBLICATION DATE

Expected May 2013

TITLE

Circum-polar overview and spatial heterogeneity of Antarctic macrobenthic communities

JOURNAL

Marine Biodiversity

SIGNIFICANCE

- This analysis suggests that all main types of macrobenthic communities are ubiquitous.
- Suspension feeders and associated fauna dominated the macrobenthic communities surveyed.

SUMMARY

The geographical coverage of a comprehensive data set on Antarctic macrobenthic communities is provided for the first time. Since the sampling methods applied since the 1950s vary considerably a robust analysis was carried out. The results show firstly, that all main types of communities, especially suspension and mobile or infaunal deposit feeders can occur everywhere. Thus, their biogeography is hardly predictable assumed to be shaped by complex biological interactions. Secondly, the often mentioned dominance of communities composed of suspension feeders and associated fauna can be confirmed.

ADDITIONAL ARTICLE

AUTHORS

V. Trouet, **H. F. Diaz (CIRES), E. R. Wahl (NESDIS/NCDC),** A. Viau, R. Graham, N. Graham, and E. R. Cook

PUBLICATION DATE

Published: April 2013

TITLE

A 1500-year reconstruction of annual mean temperature for temperate North America on decadal-to-multidecadal time scales

JOURNAL

Environmental Research Letters

SIGNIFICANCE

- Over the past 1500 years, estimated mean annual temperature for temperate North America (including most of the CONUS) was never as high as during the first decade of the 21st century.
- Authors present the first reconstruction of its kind for temperate North America that mixes annually-resolved tree ring information during the past millennium with multi-decadally resolved pollen proxy data that extends farther back in time.
- This study adds to the considerable scientific evidence that warming in the 20th century represents a clear change from prior long-term temperature trends.

SUMMARY

The authors present two reconstructions of annual average temperature over temperate North America: a tree-ring based reconstruction at decadal resolution (1200–1980 CE) and a pollen-based reconstruction at 30-year resolution that extends back to 480 CE. They maximized reconstruction length by using long but low-resolution pollen records and applied a three-tier calibration scheme for this purpose: the tree-ring based reconstruction was calibrated against instrumental annual average temperatures on annual and decadal scale; it was then reduced to a lower resolution, and was used as a calibration target for the pollen-based reconstruction. Before late-19th to early-21st century times, there are three prominent low-frequency periods in the extended reconstruction starting at 480 CE, notably the Dark Ages cool period (ca. 500–700 CE) and Little Ice Age (ca. 1200–1900 CE), and the warmer Medieval Climate Anomaly (MCA; ca. 750–1100 CE). The 9th and the 11th century are the warmest centuries and they constitute the core of the MCA in our reconstruction, a period characterized by centennial-scale aridity in the North American West. These two warm peaks are slightly warmer than the baseline period (1904–1980), but nevertheless much cooler than temperate North American temperatures during the early 21st century.

VISIT THE SCIENTIFIC PUBLICATIONS REPORT ARCHIVE

ADDITIONAL ARTICLE

AUTHORS

M. Stat, X. Pochon, E. C. Franklin, J. F. Bruno, **K. S. Casey (NESDIS/NODC),** E. R. Selig, and R. D. Gates

PUBLICATION DATE

Accepted: March 2013

TITLE

The distribution of the thermally tolerant symbiont lineage (Symbiodinium *clade D) in corals from Hawaii: correlations with host and the history of ocean thermal stress*

JOURNAL

Ecology and Evolution

SIGNIFICANCE

- The authors investigated whether thermally tolerant clade D *Symbiodinium* was in greater abundance in corals from sites with high frequencies of thermal stress anomalies.
- A significant correlation between the presence of *Symbiodinium* in clade D and a thermal history characterized by high cumulative frequency of thermal stress anomalies was found.
- This study represents the first report of clade G *Symbiodinium* in Porites lobata.

SUMMARY

Spatially intimate symbioses, such as those between scleractinian corals and unicellular algae belonging to the genus *Symbiodinium,* can potentially adapt to changes in the environment by altering the taxonomic composition of their endosymbiont communities. The authors quantified the spatial relationship between the cumulative frequency of thermal stress anomalies (TSAs) and the taxonomic composition of *Symbiodinium* in the corals *Montipora capitata, Porites lobata,* and *Porites compressa* across the Hawaiian archipelago. Sequences recovered included 2305 *Symbiodinium* ITS2 sequences from 242 coral colonies near Oahu in 2007. Sequences were grouped into 26 operational taxonomic units (OTUs) with 12 OTUs associated with *Montipora* and 21 with *Porites.* Both coral genera associated with *Symbiodinium* in clade C, and these co-occurred with clade D in *M. capitata* and clade G in *P. lobata.* The latter represents the first report of clade G *Symbiodinium* in *P. lobata.* In *M. capitata* (but not *Porites* spp.), there was a significant correlation between the presence of *Symbiodinium* in clade D and a thermal history characterized by high cumulative frequency of TSAs. The endogenous community composition of *Symbiodinium* and an association with clade D symbionts after long-term thermal disturbance appear strongly dependent on the taxa of the coral host.

VISIT THE SCIENTIFIC PUBLICATIONS REPORT ARCHIVE

ADDITIONAL ARTICLE

AUTHORS

J. Colt and **E. Kroeger (NMFS/NWFSC)**

PUBLICATION DATE

Expected 1 June 2013

TITLE

Impact of aeration and alkalinity on the water quality and product quality of transported tilapia - a simulation study

JOURNAL

Aquacultural Engineering

SIGNIFICANCE

- The authors documented the impacts of aeration type and alkalinity on important water quality parameters by using simulated hauling trials with Nile tilapia
- Results indicate that mortality due directly to hauling water quality will not be increased at high alkalinity, if pure oxygen aeration is used.
- The potential effects of water quality during hauling on survival and product quality may be less than the impacts from physical damage from loading and unloading and physiological problems resulting from pH and temperature shock during the transfer from the hauling tanks to retail holding systems.

SUMMARY

The effects of aeration and alkalinity on water quality and product quality of Nile tilapia *(Oreochrmis niloticus)* were determined for simulated commercial hauling conditions. Three types of aeration were tested: pure oxygen aeration with a fine bubble diffuser (Oxygen), air aeration with medium bubble diffusers (Air), and a combination of both pure oxygen aeration with a fine bubble diffuser and air aeration with a medium bubble diffuser (Mixed). Simulated transport hauls were conducted at two initial alkalinities: 1.74 ± 0.11 meq/L (Low) and 8.84 ± 0.55 meq/L (High). Air treatments resulted in the lowest carbon dioxide concentration, and the highest pH and un-ionized ammonia concentrations. At high alkalinities, Air treatments were unable to maintain adequate dissolved oxygen levels. Mixed treatments resulted in reduced carbon dioxide and dissolved oxygen concentrations. Oxygens treatment resulted the highest dissolved oxygen, highest carbon dioxide, and lowest pH and un-ionized ammonia. Un-ionized ammonia concentrations were higher with the High Alkalinity treatments because of higher pH. The authors observed significant mortality in Air treatments in both the Low- and High-Alkalinity treatments. Mortality in the Oxygen and Mixed treatments for both low and high alkalinities were comparable to that observed in commercial tilapia transport using fine bubble diffusers and pure oxygen.

ADDITIONAL ARTICLE

AUTHORS

M. Bunkers (NWS/RAP) and P. L. Smith

PUBLICATION DATE

Online Release: April 2013

TITLE

Comments on "An Objective High-Resolution Hail Climatology of the Contiguous United States"

JOURNAL

Weather and Forecasting

SIGNIFICANCE

- Cintineo et al. (2012) used The Weather Surveillance Radar-1988 Doppler "maximum expected size of hail" product to determine all days with hail and days with severe hail.
- The authors comment on the methods used by Cintineo et al. (2012) and describe some of the challenges in creating a radar-based hail climatology.

SUMMARY

Cintineo et al. (2012) presented a radar-based hail climatology for the continental United States (U.S.) for 2007-2010 that illustrates the advantage of multi-radar, grid-based techniques in deriving a high-resolution hail climatology. They used The Weather Surveillance Radar-1988 Doppler (WSR-88D) "maximum expected size of hail" product to determine all days with hail and days with severe hail. The size of their dataset, quality control and processing of their dataset, and results are noteworthy. For example, Cintineo et al. illustrated substantial differences between the radar-based hail climatology and the corresponding reports-only climatology, drawing into question the reliability of the reports-based climatology in some cases. While discussing challenges with using the WSR-88D data, Cintineo et al. correctly noted that beam widening is problematic in regions of single-radar coverage at long ranges from the radar. However, the authors believe that in doing so they interpreted partial beam-filling artifacts incorrectly. Partial beam filling at long ranges from the radar reduces the reflectivity, and in the case of strong storms it will spread the reduced reflectivity over a larger area than what truly exists. The authors do not contend this changes the results of Cintineo et al. in any meaningful way, but take the opportunity to clarify some of the problems associated with partial beam filling at relatively long ranges from the radar.

LINK

http://journals.ametsoc.org/doi/pdf/10.1175/WAF-D-13-00020.1

ADDITIONAL ARTICLE

AUTHORS

T.A. Warner, J.H. Helsdon, **M.J. Bunkers (NWS/RAP),** M.M.F. Saba, and R.E. Orville

PUBLICATION DATE

Expected Spring 2013

TITLE

UPLIGHTS: Upward Lightning Triggering Study

JOURNAL

Bulletin of the American Meteorological Society

SIGNIFICANCE

- Research may identify unique hazards associated with upward lightning that presently are not known or being addressed by the standards. This could have benefits for society by increasing understanding of, and safety from upward lightning from tall objects.
- This research may allow for the quantification of upward lightning as a percentage of total lightning and determination if there is a meaningful increase in upward lightning by anthropogenic activity.

SUMMARY

The UPward LIGHtning Triggering Study (UPLIGHTS) is a three-year National Science Foundation-funded field project that is taking place in Rapid City, South Dakota, from April 2012 to September 2014. Since 2004, GPS time-synchronized optical observations of upward lightning have been conducted from ten towers in Rapid City, South Dakota. These towers range in height from 91 to 191 m and are situated along an elevated ridge line that runs north south through Rapid City (Table 1, Figs. 1-2). The height of the ridge reaches approximately 180 m above the surrounding terrain. The natural conditions around Rapid City (open sky country, low height urban area, and tower locations) are favorable for optical observations of multiple towers. The working hypothesis of UPLIGHTS is that upward leaders from the towers are primarily triggered by 1) the approach of horizontally propagating negative stepped leaders associated with either intracloud development or following a +CG return stroke and/or 2) a +CG return stroke as it propagates through a previously formed leader network that is near the towers; and that specific storm types (discussed below) are favorable for upward lightning occurence. This short paper describes the background and observational elements for UPLIGHTS.

LINK

http://journals.ametsoc.org/doi/pdf/10.1175/BAMS-D-11-00252.1

ADDITIONAL ARTICLE

AUTHORS

D. R. V. Haverbeke, D. M. Stone, **L. G. Coggins, Jr. (NMFS/SEFSC),** and M. J. Pillow

PUBLICATION DATE

Expected April 2013

TITLE

Long term monitoring of an endangered desert fish and factors influencing population dynamics

JOURNAL

Journal of Fish and Wildlife Management

SIGNIFICANCE

- These results show the spring and fall abundances of native fishes, including a federally endangered species, in the lower corridor of the Little Colorado RIver in the Grand Canyon from 2001 - 2010.
- After 2006 there was an increase in relative abundance (abundance of native fish, including the endangered humpback chub, suggesting a systemwide event occurred that was beneficial to native fishes.

SUMMARY

The lower corridor of the Little Colorado River in Grand Canyon, Arizona is dominated by endemic desert fishes and is significant for conservation of these species. From 2000 to 2011, the U.S. Fish and Wildlife Service conducted biannual monitoring of native fishes in the Little Colorado River near its confluence with the Colorado River. The primary focus of these efforts was to estimate the spring and fall abundance of native fishes including the federally endangered humpback chub *Gila cypha.* From 2001 to 2006, the spring abundance estimates of chub ≥150 mm and ≥200 mm remained relatively low (≤3,419 and ≤2,002 fish, respectively). By spring 2010 these numbers were significantly higher, 8,083 and 6,250, respectively. Also from 2000 to 2006, the fall abundance estimates of humpback chub were substantially below those abundances estimated after 2006. In addition, flannelmouth sucker *Catostomus latipnnis* and bluehead sucker *C. discobolus* showed post-2006 increases in relative abundance (CPUE), suggesting a systemwide event occurred that was beneficial to native fishes. Most of these increases occurred during the spring season in the reaches of the Little Colorado River between 5 and 13.6 km upstream from the confluence. Successful production of age 0 year classes of humpback chub may be partially driven by hydrograph dynamics of the Little Colorado River, while water temperatures and predation pressures in the mainstem Colorado River likely influence survivorship of native fishes into sub-adult and adult life stages.

VISIT THE SCIENTIFIC PUBLICATIONS REPORT ARCHIVE

ADDITIONAL ARTICLE

AUTHORS

J. Demargne (NWS/OHD - no longer a NOAA employee), L. Wu (NWS/OHD), S. Regonda (NWS/OHD), J. Brown, **H. Lee (NWS/OCCWWS)** M. He, D. J. Seo, **R. Hartman (NWS/OCCWWS), H. Herr (NWS/OHD), M. Fresch (NWS/OHD),** J. Schaake[9], **Y. Zhu (NWS/OCCWWS)**

PUBLICATION DATE

Expected July or August 2013

TITLE

The Science of NOAA's Operational Hydrologic Ensemble Forecast Service

JOURNAL

Bulletin of the American Meteorological Society

SIGNIFICANCE

- NOAA's National Weather Service (NWS) is implementing a short- to long-range Hydrologic Ensemble Forecast Service (HEFS).
- A key component of HEFS ingests weather and climate forecasts from multiple Numerical Weather Prediction models to produce seamless and bias-corrected precipitation and temperature ensembles at the hydrologic basin scale.

SUMMARY

The HEFS addresses the need to quantify uncertainty in hydrologic forecasts for flood risk management, water supply management, streamflow regulation, recreation planning, and ecosystem management, among other applications. The HEFS extends the existing hydrologic ensemble services to include short-range forecasts, incorporate additional weather and climate information, and better-quantify the major uncertainties in hydrologic forecasting. It provides, at forecast horizons ranging from 6-hr to about a year, ensemble forecasts and verification products that can be tailored to users' needs. Based on separate modeling of the input and hydrologic uncertainties, the HEFS includes: 1) the Meteorological Ensemble Forecast Processor, which ingests weather and climate forecasts from multiple numerical weather prediction models to produce bias-corrected forcing ensembles at the hydrologic basin scales; 2) the Hydrologic Processor, which inputs the forcing ensembles into hydrologic, hydraulic, and reservoir models to generate streamflow ensembles; 3) the hydrologic Ensemble Post-processor, which aims to account for the total hydrologic uncertainty and correct for systematic biases in streamflow; 4) the Ensemble Verification System, which verifies the forcing and streamflow ensembles to help identify the main sources of skill and error in the forecasts; and 5) the Graphics Generator, which enables forecasters to create a large array of ensemble and related products. Examples of verification results from multi-year hindcasting illustrate the expected performance and limitations of HEFS. Finally, future scientific and operational challenges to fully embrace and practice the ensemble paradigm in hydrology and water resources services are discussed.

HEFS provides, for short- to long-range, uncertainty-quantified forecast and verification products. Evaluation of the HEFS through multi-year hindcasting and large sample verification is currently underway and results obtained so far show positive skill and reduced bias in the short- to medium-term when compared to climatology-based ensembles and single-valued forecasts.

VISIT THE SCIENTIFIC PUBLICATIONS REPORT ARCHIVE

AUTHORS

D. M. Van Doornik, D. L. Eddy, **R. S. Waples,** S. J. Boe, T. L. Hoffnagle, **E. A. Berntson,** and **P. Moran (NMFS/NWFSC)**

PUBLICATION DATE

Expected May 2013

TITLE

Genetic monitoring of threatened chinook salmon populations: estimating introgression of non-native hatchery stocks and temporal genetic changes

JOURNAL

North American Journal of Fisheries Management

SIGNIFICANCE

- Artificial propagation of salmonids has long been used in attempts to increase their abundance and to conserve threatened populations. Such practices, however, carry certain genetic risks to the native populations in the area.
- Most of the native populations of Chinook salmon sampled in northeast Oregon do not show negative genetic effects of supplementation efforts in that area. However, two populations do show evidence of genetic introgression of a non-native hatchery stock.

SUMMARY

Conservation efforts aimed at Pacific salmon *(Oncorhynchus* spp.) populations have frequently utilized artificial propagation in an attempt to increase fish abundance. However, this approach carries the risk of unwanted changes in genetic characteristics of the target population, and perhaps others that might incidentally be affected. We used genetic monitoring techniques to estimate the amount of introgression that has occurred from non-native hatchery stocks into native populations and to determine the extent of genetic changes that have occurred in association with supplementation efforts over the past 20-50 years in Snake River chinook salmon *(O. tshawytscha)* populations from northeast Oregon. A total of 4,178 fish from 13 populations were genotyped for 12 microsatellite DNA loci. Expected heterozygosity values for each sample ranged from 0.707 – 0.868. Estimates of the effective number of breeders per year in the naturally spawning populations ranged from 20.6 - 459.1, whereas in the hatchery populations, they ranged from 33.8 – 1,118.8. We found that introgression from the Rapid River Hatchery stock was particularly noticeable in the early 1990s, but it appears to have had a substantial effect on only two of the native populations (Lookingglass Creek and Upper Grande Ronde River), despite the ample opportunities that existed for introgression to occur. All seven of the native populations sampled have maintained their levels of within population genetic diversity throughout the sampling period. Overall, this region's supplementation efforts appear to have had a minimal effect on the genetic diversity of its chinook salmon populations.

AUTHORS

T. C. Wainwright and **L. A. Weitkamp (NMFS/NWFSC)**

PUBLICATION DATE

Expected Summer 2013

TITLE

Effects of climate change on Oregon coast coho salmon: habitat and life-cycle interactions

JOURNAL

Northwest Science

SIGNIFICANCE

- As cold water fishes, climate change is unlikely to benefit coho salmon (or other Pacific salmon).
- Despite substantial uncertainties and variations in effects among populations, the large number of observed negative impacts from climate change indicates a significant climate-driven risk to sustainability of these populations.
- The best strategy for sustainable salmon given negative expectations from climate change is maximizing resilience of all habitats used by salmon and promoting fish diversity.

Coho Salmon

SUMMARY

Coho salmon *(Oncorhynchus kisutch)* populations spawn in the coastal rivers of Oregon, and once supported robust fisheries, however they are now listed as a "threatened species" under the U.S. Endangered Species Act. Climate change is an increasing concern in salmon conservation, and this study assesses the effects of climate change on sustainability of these populations. Four distinct habitats are important to different life-history stages of coho salmon: terrestrial forests, freshwater rivers and lakes, estuaries, and the ocean. Each of these habitats is affected by multiple aspects of climate change, resulting in a complex web of pathways influencing sustainability. The authors summarize regional climate change studies to predict future climate patterns affecting these habitats, identify the ecological pathways by which these patterns affect coho salmon, and review coho salmon ecology to assess the likely direction and magnitude of population response. Despite substantial uncertainties in specific effects and variations in effects among populations, the preponderance of negative effects throughout the life cycle indicates a significant climate-driven risk to future sustainability of these populations. We recommend that management policies for all four habitats focus on maximizing resilience to the effects of climate change as it interacts with other natural and anthropogenic changes.

AUTHORS

L. E. Woodson, B. K. Wells, P. K. Weber, **R. B. MacFarlane,** G. E. Whitman, and R. C. Johnson **(NMFS/SWFSC)**

PUBLICATION DATE

Expected Spring/Summer 2013

TITLE

Selective mortality on length, growth rate and rearing origin of juvenile chinook salmon (Oncorhynchus tshawytscha)

JOURNAL

Marine Ecology Progress Series

SIGNIFICANCE

- The authors detected a significant effect of both size and growth-rate selective mortality on juvenile Central Valley fall-run Chinook salmon.
- The effect appears independent of fish rearing origin, and was only detected in a year of poor ocean conditions with low food availability and lower survival to adulthood.
- This significant mortality event preceded devastatingly poor adult returns in 2007, which then led to complete closures of the salmon fisheries off California in 2008 and 2009.

SUMMARY

Selective mortality during early life history stages can have significant population-level consequences, yet critical periods when selective mortality occurs, the strength of selection, and under what environmental conditions can be difficult to identify. Here, the authors used otolith microstructure and chemistry to examine factors potentially linked to selective mortality of juvenile fall-run Chinook salmon *(Oncorhynchus tshawytscha)* from California's Central Valley during early ocean residence. Back-calculated size and growth rates of the population were compared across three sample periods: as juveniles exited the San Francisco Bay estuary (estuary-exit), after their first month at sea (summer-ocean), and five months after ocean entry (fall-ocean). We compared mortality dynamics during years of exceptional recruitment (addition of individuals to harvestable population; 2000 and 2001) to a year of poor recruitment (2005). Otoliths from 2005 were also analyzed for sulfur isotopes to discern hatchery from naturally spawned stock. Significant size and growth-rate selective mortality were detected during the first month at sea in the low recruitment year of 2005, but not in 2000/2001. Individuals that were larger and growing faster during freshwater and estuarine rearing were more likely to survive to summer and fall in the low recruitment year. There was a slight, but insignificant, increase in the proportion of hatchery to naturally spawned individuals from estuary-exit to fall-ocean, suggesting fish from neither origin was overwhelmingly favored. Their results suggest that Central Valley Chinook salmon can be subject to significant size and growth-rate selective mortality resulting in low adult abundance, and this mortality appears independent of origin.

Juvenile Chinook Salmon

AUTHORS

J. McMillan, F. Orth, **M. Liermann,** J. Starr, **G. Pess,** and X. Augerot **(NMFS/NWFSC)**

PUBLICATION DATE

Accepted: March 21, 2013

TITLE

Using a stream network census of fish and habitat to assess models of juvenile salmonid distribution

JOURNAL

Transactions of the American Fisheries Society

SIGNIFICANCE

- The authors censused juvenile salmonids and stream habitat over two consecutive summers to test the ability of habitat models to explain the distribution of juvenile salmonids
- Extrapolation of juvenile salmon-freshwater habitat relationships should be done with caution and should include variables associated with the river system and the location within a river system
- The association between freshwater habitat and salmonids varies according to the stream and the location of habitat within a stream more than the habitat and characteristics, making it difficult to extrapolate juvenile salmon- freshwater habitat relationships.

SUMMARY

The authors censused juvenile salmonids and stream habitat over two consecutive summers to test the ability of habitat models to explain the distribution of juvenile coho salmon *Oncorhynchus kisutch*, young-of-the-year (age 0) steelhead *Oncorhynchus mykiss*, and steelhead parr (≥ age 1) within a network consisting of several different sized streams. The authors network-scale habitat models explained 27%, 11%, and 19% of the variation in the density of juvenile coho salmon, age 0 steelhead, and steelhead parr, respectively, but strong levels of spatial autocorrelation were typically present in the residuals. Explanatory power of base habitat models increased and spatial autocorrelation decreased with sequential inclusion of variables accounting for the effects of stream size, year, stream, reach location and a tertiary interaction term. Stream-scale models were highly variable. Fish-habitat associations were rarely linear and ranged from negative to positive, and the variable accounting for location of the habitat within a stream was often more important than habitat. The limited success of the network-scale models was apparently related to variation in the strength and shape of fish-habitat associations across and within streams and years. These results indicate it there are several potential limitations to extrapolating models to broader areas based only on spatially limited surveys.

AUTHORS

J. R. Ray (NOS/NGS), P. Rebischung, and R. Schmid

PUBLICATION DATE

Published: 2013

TITLE

Dependence of IGS products on the ITRF datum

JOURNAL

Reference Frames for Applications in Geosciences - International Association of Geodesy Symposia

SIGNIFICANCE

- This paper reviews the historic relationships between Global Navigation Satellite System (GNSS) terrestrial reference frames, International GNSS Service (IGS) products, and the International Terrestrial Reference Frame (ITRF) datum (i.e., origin, orientation, and scale).
- Recommendations are made for future reference frame updates to ensure stability and to minimize user inconvenience.

SUMMARY

Throughout its nearly two decades, the International GNSS (Global Navigation Satellite Systems) Service (IGS) has sought to align its products closely to successive realizations of the International Terrestrial Reference Frame (ITRF). During the past decade, IGS impacts due to ITRF updates have been smaller and mostly caused by errors in the results from the contributing space geodetic techniques. Frame orientations (rotations) are purely conventional, so the IGS relies on the ITRF via a subset of reliable, globally distributed stations. Except for the period when ITRF93 was used, this procedure has worked well. The IGS origin in principle could be self-reliant or contributory to ITRF by direct observation of a frame origin aligned to the long-term center of mass of the entire Earth system. In practice, however, GNSS-based results have been less reliable than those from satellite laser ranging (SLR). Until the transition from ITRF2005 to ITRF2008, there have sometimes been significant origin shifts as SLR results have evolved. However, the present stability of the ITRF origin may finally have reached the few-mm level. In many respects, the IGS dependence on the ITRF scale is most subtle and problematic. In addition to an overall Helmert alignment of the IGS frame to match the ITRF scale (and other datum parameters), since 2006 the IGS calibration values for the GNSS satellite antenna z-offsets depend directly on the same ITRF scale (due to high correlations if the IGS frame scale is not fixed). We therefore face a non-linear situation to maintain full consistency between all IGS products and the ITRF scale: each IGS frame contribution to ITRF based on one set of antenna calibrations must be used, together with frames from other techniques, to determine an updated ITRF and new antenna calibrations, which are then no longer strictly consistent with the starting IGS frame. Only SLR and very long baseline interferometry (VLBI) have been considered reliable and accurate enough to be used for the ITRF scale. But experience and theoretical studies have shown that neither is accurate to better than about 1ppb. Consequently, the authors strongly urge that the ITRF scale hereafter be fixed conventionally to the ITRF2008 scale indefinitely until it is convincingly shown that VLBI and/or SLR can determine the ITRF scale within 0.5ppb. If this is not done, the IGS might maintain its own ITRF2008 scaled frame to minimize future operational dislocations.

AUTHORS

D. A. Smith, M. Veronneau, **D. R. Roman,** J. Hugang, Y. M. Wang, **M. G. Sideris (NOS/NGS)**

PUBLICATION DATE

Published: 2013

TITLE

Towards the unification of the vertical datum over the North American continent

JOURNAL

Reference Frames for Applications in Geosciences - International Association of Geodesy Symposia

SIGNIFICANCE

- Authors discuss the ongoing work of geodetic agencies throughout North America to create a new, unified vertical datum for the continent, which could replace the North American Vertical Datum of 1988.
- The authors propose a detailed description of the definition, realization, and maintenance of the datum, and discuss the challenges in realization and maintaining the datum.

SUMMARY

The United States adopted the North American Vertical Datum of 1988 (NAVD 88) as its official vertical datum in the 1990s. Canada has been using the Canadian Geodetic Vertical Datum (CGVD28) for its height applications since the 1930s. The use of different datums causes inconsistent heights across the border between the two countries, and the topographic height data from the two countries are not compatible. Both datums rely on passive control and significant pre-modern survey data, yielding not only misalignment of the datums to the best known global geoid at approximately 1-2 m, but also local uplift and subsidence issues which may significantly exceed 1-2 m in extreme cases. Today, the Global Navigation Satellite System (GNSS) provides the geometric (ellipsoidal) height to an accuracy of 1-2 cm globally. Because of this increased accuracy, users have begun to demand a physical height system that is closely related to the Earth's gravity field to a comparable accuracy. To address this need, government agencies of both countries are preparing the next generation of vertical datums. To avoid inconsistencies, it is in the interest of both countries to have a united, seamless, highly accurate vertical datum. The proposed replacements for CGVD28 and NAVD88 will be based on GNSS positioning and a high accuracy gravimetric geoid that covers the territories of the United States, Canada, Mexico and the surrounding waters (to include all of Alaska, Hawaii, the Caribbean and Central America). The datum will also account for the effect of the sea level change, postglacial rebound, earthquakes and subsidence, by providing information on these changes.

IOPscience iopscience.iop.org

Home Search Collections Journals About Contact us My IOPscience

A 1500-year reconstruction of annual mean temperature for temperate North America on decadal-to-multidecadal time scales

This article has been downloaded from IOPscience. Please scroll down to see the full text article.

2013 Environ. Res. Lett. 8 024008

(http://iopscience.iop.org/1748-9326/8/2/024008)

View the table of contents for this issue, or go to the journal homepage for more

Download details:
IP Address: 155.206.113.46
The article was downloaded on 11/04/2013 at 16:38

Please note that terms and conditions apply.

VISIT THE SCIENTIFIC PUBLICATIONS REPORT ARCHIVE

OPEN ACCESS
IOP PUBLISHING ENVIRONMENTAL RESEARCH LETTERS
Environ. Res. Lett. **8** (2013) 024008 (10pp) doi:10.1088/1748-9326/8/2/024008

A 1500-year reconstruction of annual mean temperature for temperate North America on decadal-to-multidecadal time scales

V Trouet[1], H F Diaz[2], E R Wahl[3], A E Viau[4], R Graham[5], N Graham[5] and E R Cook[6]

[1] University of Arizona, LTRR, Tucson, AZ 85721-0058, USA
[2] NOAA/CIRES/PSD1, 325 Broadway, Boulder, CO 80305, USA
[3] NOAA/NCDC/Paleoclimatology, 325 Broadway, Boulder, CO 80305, USA
[4] University of Ottawa, LPC, Ottawa, ON, K1N 6N5, Canada
[5] Hydrologic Research Center, San Diego, CA 92130, USA
[6] Tree Ring Lab, Lamont-Doherty Earth Observatory, Palisades, NY 10964-8000, USA

E-mail: trouet@ltrr.arizona.edu

Received 14 December 2012
Accepted for publication 26 March 2013
Published 11 April 2013
Online at stacks.iop.org/ERL/8/024008

Abstract

We present two reconstructions of annual average temperature over temperate North America: a tree-ring based reconstruction at decadal resolution (1200–1980 CE) and a pollen-based reconstruction at 30 year resolution that extends back to 480 CE. We maximized reconstruction length by using long but low-resolution pollen records and applied a three-tier calibration scheme for this purpose. The tree-ring-based reconstruction was calibrated against instrumental annual average temperatures on annual and decadal scale, it was then reduced to a lower resolution, and was used as a calibration target for the pollen-based reconstruction. Before the late-19th to the early-21st century, there are three prominent low-frequency periods in our extended reconstruction starting at 480 CE, notably the Dark Ages cool period (about 500–700 CE) and Little Ice Age (about 1200–1900 CE), and the warmer medieval climate anomaly (MCA; about 750–1100 CE). The 9th and the 11th century are the warmest centuries and they constitute the core of the MCA in our reconstruction, a period characterized by centennial-scale aridity in the North American West. These two warm peaks are slightly warmer than the baseline period (1904–1980), but nevertheless much cooler than temperate North American temperatures during the early-21st century.

Keywords: temperature, tree ring, pollen, North America, medieval climate anomaly, Little Ice Age

1. Introduction

Growing concern about ongoing and projected climatic change raises questions about anthropogenic forcing of the climate system and the amplitude of its response. Improving our understanding of the climate system's sensitivity and its natural variability requires a longer time frame than instrumental data alone can offer. Moreover, knowledge of pre-industrial climate conditions is important to distinguish between anthropogenic and natural drivers of climatic variability. Proxy climate records, derived from geological, biological, and documentary archives, have therefore been

Content from this work may be used under the terms of the Creative Commons Attribution 3.0 licence. Any further distribution of this work must maintain attribution to the author(s) and the title of the work, journal citation and DOI.

 © 2013 IOP Publishing Ltd Printed in the UK

VISIT THE SCIENTIFIC PUBLICATIONS REPORT ARCHIVE

developed to reconstruct past climate at a wide range of spatial and temporal scales. Due to the high density of available high-resolution climate proxy records and boundary conditions that are comparable to the present, the Late Holocene (here defined as the most recent ∼2000 years) has been the focus of an ever-growing body of paleoclimate research (e.g., Wanner *et al* 2008, Jones *et al* 2009).

Hemispheric or global average temperature variability has been a dominant recent focus of Late Holocene climate reconstructions using high-resolution proxy records (e.g., Mann *et al* 2009, Frank *et al* 2010). In general, the last 2000 years depict four contrasting periods before late-19th to early-21st century times: the Roman Warm Period (RWP; about 0–400 CE), the Dark Ages Cool period (DAC; about 400–700 CE), the medieval climate anomaly (MCA; about 800–1200 CE), and the Little Ice Age (LIA; about 1300–1850 CE). Our study explores climate over the last 2000 years, but the reader is referred to the chapter on paleoclimate in the 2007 Intergovernmental Panel on Climate Change assessment report (IPCC AR4; Jansen *et al* (2007) and references therein) for a more complete overview of the Holocene and earlier paleoclimate history.

The LIA has been studied extensively and recent studies have hypothesized that this relatively cool period was more or less homogeneous in space and time across the globe (Mann *et al* 2008, Kaufman *et al* 2009, Mann *et al* 2009, Christiansen and Ljungqvist 2012, Ljungqvist *et al* 2012), although its start appears to have been temporally offset in different sub-continental regions (cf Wahl *et al* 2012, PAGES2K_consortium 2013). The spatio-temporal coherency of the two earlier warm periods (RWP and MCA) and cool DAC remains a topic of extensive scientific debate (e.g., Bradley *et al* 2003, Berglund 2003, Diaz *et al* 2011). Moreover, amongst these earlier periods, the well-documented MCA has been proposed as a benchmark period for distinguishing between natural and anthropogenic forcings. This has recently encouraged several independent large-scale regional climate proxy syntheses and modeling studies aimed at unraveling the dynamics behind the regional climate patterns reconstructed during the MCA (Graham *et al* 2007, Mann *et al* 2009, Trouet *et al* 2009, Graham *et al* 2011).

The development of more regional-scale temperature reconstructions covering the last 2000 years is needed to address the spatio-temporal patterns of the RWP, DAC, MCA, and LIA (IPCC 2007). Following the IPCC AR4 recommendations, this has been one of the main objectives set by the science and implementation strategy of the Past Global Changes (PAGES) Programme of the International Geosphere Biosphere Programme (IGBP), summarized in IGBP Report 57 under Focus 2, 'Regional Climate Dynamics Theme 2'.

In this study, we describe an effort to produce a long (∼480–1980 CE) annual temperature reconstruction for temperate North America at decadal-to-multidecadal resolution by combining tree-ring records with a network of fossil lake pollen sites across most of North America. Tree-ring records have annual resolution, and provide absolute dating, but long-lived (500+ years) temperature-sensitive trees are largely restricted to the western half of the continent. Climate-sensitive pollen records can be used to extend tree-ring-based temperature reconstructions back in time, but they are often limited in temporal resolution (decadal- to centennial-scale) and can be affected by age model uncertainty and therefore do not generally allow direct calibration against high-resolution instrumental records.

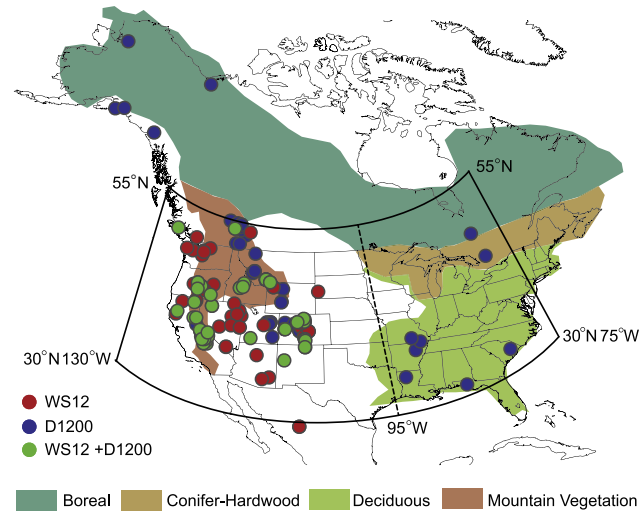

Figure 1. Map identifying the tree-ring network (dots) used in the reconstructions for the period 1200–1980 CE (WS12, 1200-on, and common records); the spatial domains of the pollen eco-region reconstructions (using the Fedorova *et al* (1994) classification scheme, color polygons), from which predictor time series were derived to extend the tree-ring-based reconstructions prior to 1200 CE; and the target region (solid black lines) of the merged (pollen + trees) temperature reconstruction. Dotted line delimits the western target region represented by the annual-scale tree ring-based reconstructions (WS12 and 1200-on).

In the following, we describe the methodology used to combine these two types of data sets to develop our temperate North America temperature reconstructions, offer a discussion of the main characteristics of our reconstructions, and compare our results with other studies of regional and hemispheric-scale temperature reconstructions.

2. Data and methods

We applied a three-tier calibration scheme to allow for temperature calibration of the pollen records that were sampled at a 30 year resolution: a tree-ring-based reconstruction (1200–1980 CE) was calibrated against instrumental annual average temperatures on (1) an annual and (2) a decadal scale; this was then reduced to a significantly lower resolution using a ∼110 year LOWESS smoothing algorithm and sampled at the same 30 year time step as the pollen-based data; and (3) used as a calibration target for the pollen-based reconstruction. All reconstructions are expressed as anomalies from a 1904–1980 reference period.

2.1. The high-resolution (interannual to decadal scale) series

For the high-resolution component of the reconstruction, we combined two semi-independent tree-ring data sets (with

VISIT THE SCIENTIFIC PUBLICATIONS REPORT ARCHIVE

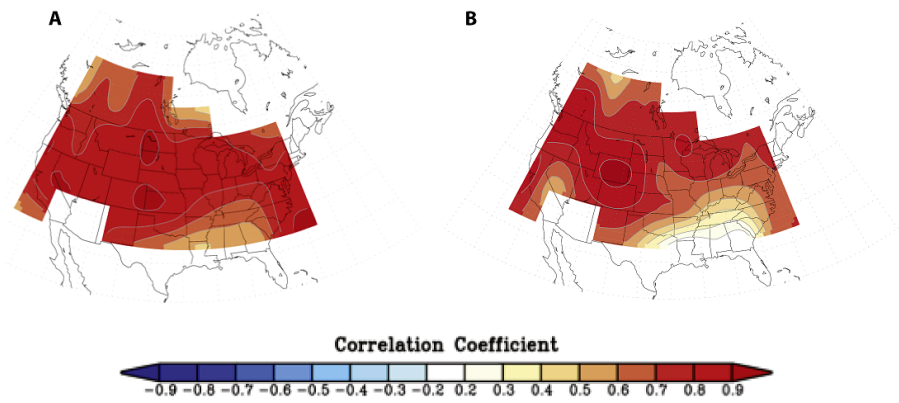

Figure 2. Spatial Pearson correlation maps of decadal averages of spatial mean of WS12 (A) and 1200-on (B) reconstructions with gridded decadal averages of annual average temperature fields derived from the NOAA merged land–ocean surface temperature (MLOST) data set (V3.5.1; Smith *et al* 2008). Correlations were calculated over the period 1880–1979 ($n = 10$) and are significant ($p < 0.05$) for $|r| > 0.632$. (NOAA merged air land and SST Anomalies data provided by the NOAA/OAR/ESRL PSD, Boulder, Colorado, USA, from their web site at www.esrl.noaa.gov/psd/. These data are also available in annualized and seasonalized forms from NOAA's National Climatic Data Center at www.ncdc.noaa.gov/paleo/pubs/pcn/pcn-MLOST.html).

Table 1. Reconstruction and calibration characteristics.

Reconstruction	Period (CE)	Resolution	Calibration target	Calibration period (CE)	Region
WS12	1500–1980	Annual	HADCRUT3v	1875–1980	30°–55°N, 95°–130°W
1200-on	1200–1987	Annual	HADCRUT3v (infilled)	1850–1987	30°–55°N, 95°–130°W
D1200	1200–1980	Decadal	HADCRUT3v (infilled)	1850–1980	30°–55°N, 75°–130°W
NAM480	480–1950	Tri-decadal	D1200	1200–1950	30°–55°N, 75°–130°W

approximately 30% overlap in contributing series; figure 1). A first set (table 1) includes chronologies from sites in an area of western mid-latitude North America bounded by 30°–55°N, 95°–130°W, with one additional chronology in west-central Mexico (see also Wahl and Smerdon (2012) for details). The proxy records in this data set were calibrated and validated at an interannual scale using the HadCRUT3v 5° × 5° gridded surface annual temperature data for the selected region for the period 1875–1980 CE (Wahl and Smerdon (2012), cf SOM). The resulting annual temperature reconstruction, hereafter referred to as WS12, covers 1500–1980 CE for the western temperate region of North America, illustrated in figure 1 (portion of solid-outlined region west of dashed line at 95°W). We used a second tree-ring data set to extend the original WS12 reconstruction back in time (1200–1987 CE); this second proxy set included records over a wider area of North America (figure 1; data and metadata available as part of the PAGES 2K Temperature Synthesis data set at www.ncdc.noaa.gov/paleo/paleo.html, PAGES2K_consortium 2013). It was calibrated and validated in the same manner as WS12 over the period 1850–1987 using the Mann *et al* (2009) in-filled version of the same instrumental record (PAGES2K_consortium 2013, cf supplementary online material (SOM)), allowing gridded information in the third quarter of the 19th century to be employed for validation that was not available when the WS12 reconstruction was developed. The resulting reconstruction is hereafter referred to by the term '1200-on'.

The WS12 and 1200-on time series are well validated, with r^2-values between spatially averaged instrumental and reconstructed values over the validation period of 0.423 and 0.421, respectively, and differences between instrumental and reconstructed validation period spatially averaged temperatures of −0.022 °C and 0.013 °C, respectively (relative to mean values of −0.352 and −0.258, respectively). The 1200-on time series, however, exhibits lower skill (here evaluated using reduction of error (RE) and coefficient of efficiency (CE) statistics; Cook *et al* 1994), particularly at the grid-scale level, than the shorter WS12 reconstruction. WS12 exhibits validation grid-scale RE, spatial-mean RE, and spatial-mean CE of 0.40, 0.62, and 0.42, respectively, while the 1200-on reconstruction exhibits 0.13, 0.53, and 0.31 for the same measures. Decreasing reconstruction skill has previously been noted for other reconstructions that use sequentially nested calibrations as a function of record length back in time (e.g., Cook *et al* 2004). We thus used WS12 as the reconstruction for 1500–1980 and joined the 1200-on reconstruction to it to cover the period 1200–1499. To ensure comparability across the splice at 1500, we regressed WS12 onto the 1200-on reconstruction over the 1500–1980 period, and then used this regression and the 1200-on reconstructed values to fit (scale) WS12-consistent values for the western spatial mean of the target region (west of the dotted line in figure 1) during 1200–1499. Annual detail and comparison of the WS12 and 1200-on reconstructions is provided in the appendix.

For reconstruction at the decadal scale, a larger area of temperate North America, extending from 75° to 130° W over the same latitudinal range (figure 1), is considered an appropriate regional target, as indicated by the spatial

VISIT THE SCIENTIFIC PUBLICATIONS REPORT ARCHIVE

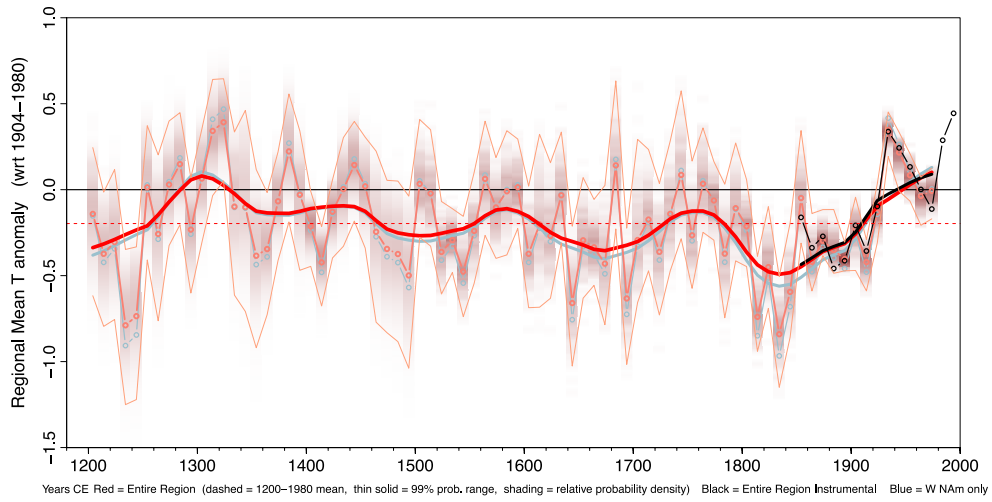

Figure 3. Decadal-scale, tree-ring-based reconstruction (D1200) of annual mean temperature deviations from a 1904 to 1980 average (solid black line) for temperate North America (30°–55°N, 75°–130°W; red) and western North America (30°–55°N, 95°–130°W; blue). Values shown are decadal means and a $f = 1/7$ (∼110 year) lowess filter was applied to highlight low-frequency fluctuations. The average for the full period of record (1200–1980) is shown as a dotted red line, variable shading gives relative probability density for each decadal mean value, thin red lines denote 99% probability range associated with each decadal value.

correlation maps between the decade-averaged spatial-mean time series of WS12 and 1200-on and decadal averages of the instrumental annual temperatures for each grid box (figure 2). These correlations indicate that the western North America reconstruction captures the essential features of spatio-temporal variability in this domain over the instrumental period at decadal scale, and also captures substantial spatial variability at this time scale over the larger continental region east to 75°W, with the exception of the southeastern United States. Decadal averages of the spliced annual-scale 1200–1980 reconstruction were therefore used as predictors in a calibration against instrumental decadal averages of annual temperatures over the full target region (30°–55°N, 75°–130°W), for a period covering 1850–1980, with very high skill ($r^2 = 0.93, p < 0.01, n = 13$, using the in-filled instrumental HadCRUT3v data set of Mann *et al* (2009)). Finally, this calibration fit was used to reconstruct decadal averages of annual temperature for the entire 1200–1980 period ($n = 78$). In both the annual and decadal reconstructions, the fitted values were scaled so that their variance matched that of the target data during the fitting period. The results are shown in figure 3, where the red (blue) curves give the full (western) North American expected value (EV) reconstructions, and the black curve shows the 1850–2000 CE full North American instrumental values.

Uncertainty for the spliced reconstruction was estimated using probabilistic uncertainty ensembles ($n = 1000$) generated using bootstrapped realizations of the regression residuals for both the WS12 and the 1200-on reconstructions (cf Wahl and Smerdon 2012). All realizations were modeled to have the same autoregressive characteristics as the residuals in the original regression. The process described above to derive the EV decadal reconstructions was then repeated in a two-step Monte Carlo design across the possible combinations of five hundred WS12 and five hundred 1200-on ensemble members (500 realizations of the 1200-on reconstruction matched with each of the 500 realizations of the WS12 reconstruction). It is important to note that the probability ranges estimated by this analysis (from the percentiles of the Monte Carlo output, figure 3) are calculated for the decadal means and thus are significantly narrower than the corresponding ranges that would be expected for annual values, from theory of the standard error of the mean. The resulting average of the 95% probability ranges for each decade in the 1200–1499 and 1500–1980 periods of the decadal-scale 1200–1980 reconstruction are 0.58 °C and 0.44 °C, respectively, and are thus 1.3 times higher for the 1200–1499 period compared to 1500–1980.

2.2. The lower resolution (tri-decadal scale) series

In a next step, we extended the tree-ring-based decadal-scale mean annual temperature reconstruction (hereafter named D1200 for decadal-1200) back to 480 CE at a 30 year resolution using pollen data for the regions of North America indicated in figure 1. For this purpose, we performed a principal component analysis (PCA) on four regional composite temperature reconstructions (360–1950 CE; Viau *et al* 2012) that were based on a network of pollen sequences from deciduous, hardwood, boreal, and mountain eco-regions of North America (figure 1). Regional composite reconstructions using pollen sequences have been shown to increase temporal resolution and reduce dating concerns of individual site reconstructions (Viau *et al* 2006, 2012). Moreover, high-resolution varved-lake sediments confirm that low and high-frequency changes are recorded in pollen sedimentary sequences during the past 2000 years in eastern North America (Wahl *et al* 2012, Gajewski 1987, 1988) and continental-scale North America (Viau *et al* 2006). The prairie eco-region reconstruction for central North America was not used because its vegetation response to climate change appears mainly controlled by precipitation (Viau *et al*

VISIT THE SCIENTIFIC PUBLICATIONS REPORT ARCHIVE

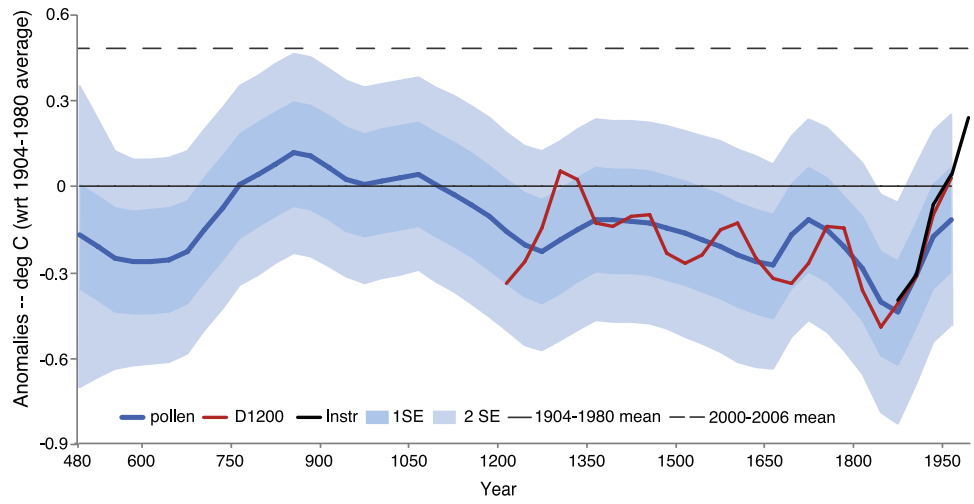

Figure 4. Reconstruction (NAM480; dark blue curve) of 30 year averages of annual mean temperature deviations from a 1904 to 1980 average for temperate North America (30°–55°N, 75°–130°W; full black horizontal line). Values shown correspond to the combination of three pollen-reconstruction PCs resulting from a stepwise multiple linear regression with the 30 year-subsampled D1200 lowess temperature series (red curve), and thus reflect low-frequency variations. Light (medium) blue zones indicate 2SE (1SE) uncertainty estimations (as explained in text) associated with each 30 year value. Black curve shows comparably smoothed instrumental temperature values up to 1980. The dashed black line represents the average temperature deviation of the comparably smoothed instrumental data for the period 2000–2006.

2012). In our study, the regional mean annual temperature reconstructions were resampled at 30 year intervals to compare to D1200. For a more direct comparison to D1200, we used mean annual temperature reconstructions rather than summer temperature anomalies as in Viau *et al* (2012).

The resulting PCA scores (360–1950 CE; $n = 54$) were then included in a stepwise multiple linear regression against D1200. For this purpose, D1200 was smoothed using a ∼110 year lowess filter and sampled every third decade to approximate the time scale and sampling resolution of the pollen-based reconstructions. Three combined PC axes explaining 87% of the common variance in the four pollen reconstructions were retained in the stepwise regression and explained 33.4% of the variance in D1200. This tri-decadal pollen-based reconstruction is designated NAM480 (for North America 480 CE).

For NAM480, uncertainty bands were estimated to reflect error due to the pollen regional reconstruction process and error in the regression model of the pollen-based time series against D1200. Regression error (1) was estimated as 1 and 2 standard error (SE) units of the regression model of the predicted y-value (D1200) for an individual predictor x (pollen-based time series). Additional uncertainty to account for the fact that the predictor (pollen-based time series; x) variables are effectively probabilistic estimates of the true population of x values (2) was estimated based on the 1SE and 2SE limits for the four contributing regional pollen-based reconstructions. The SEs for the regional reconstructions were developed using a Monte Carlo resampling technique that generated random pollen-based reconstructions by sampling values at each time step of the individual pollen-based series within their uncertainty limits (Viau *et al* 2006). This process was repeated 10 000 times to generate the regional reconstruction uncertainty bands. These uncertainty bands were then entered into the previously developed PCA and multiple linear regression equations to determine the component of the overall 1SE and 2SE uncertainty limits that was inherent to the regional pollen-based reconstruction method.

Further additional uncertainty due to the related fact that the predictand (D1200; y) variables are similarly probabilistic estimates of the true population of y values (3) was estimated by the SE of the smoothed predictand time series. For this purpose, a ∼110 year lowess filter was applied to each of the 250 000 ensemble members of the D1200 reconstruction (see uncertainty calculation description in section 2.1). Estimated standard deviations were then calculated across the ensemble members for each decade, and averaged over the entire reconstruction period (1200–1980). Finally, the squares of the three (assumed independent) errors were added and the square root of this sum was taken as an estimation of total error. Due to the resampling of the regional pollen-based reconstructions at 30 year intervals (for comparison to D1200), reliable SE uncertainty bands were only available from 480 CE onwards, leading us to truncate our reconstruction at this date.

3. Results and discussion

We developed two reconstructions of annual average temperature over temperate North America: a tree-ring-based reconstruction that is presented at decadal resolution and covers the period 1200–1980 CE (D1200; figure 3) and a pollen-based reconstruction sampled at a 30 year resolution that extends back to 480 CE (NAM480; figure 4). We maximized reconstruction length by applying a three-tier calibration scheme to long but low-resolution pollen records. This approach allowed us to provide a temperature calibration for the pollen records, for which the instrumental data record provides too few data points (the period 1850–2010 only includes five 30 year periods). NAM480

VISIT THE SCIENTIFIC PUBLICATIONS REPORT ARCHIVE

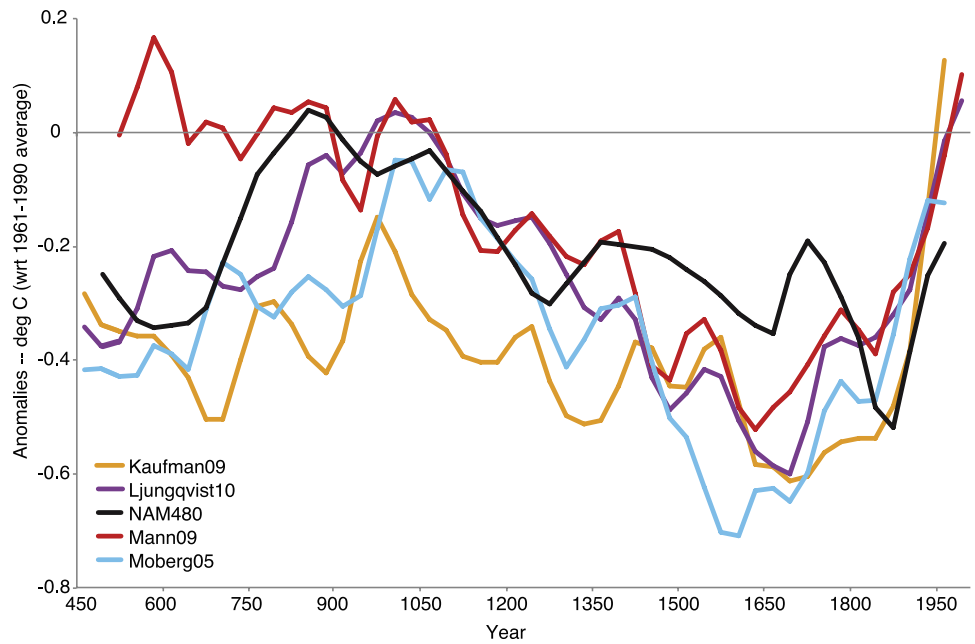

Figure 5. Comparison of the tri-decadal annual temperature reconstruction for temperate North America (NAM480; this letter) with three hemispheric-scale temperature reconstructions (Mann *et al* 2009, Ljungqvist 2010, Moberg *et al* 2005) and one temperature reconstruction for the Arctic region (Kaufman *et al* 2009) that cover the same time period. Original annual resolution reconstructions were reduced to 30 year resolution in the same way as our reconstruction (see section 2). All reconstructions are shown as deviations from a 1961 to 1990 average.

represents a reasonable calibration of the PCA time series from four regional pollen-based reconstructions against the low-frequency component of D1200 (figure 4). The smoothed/subsampled D1200 values fall nearly entirely within the NAM480 one standard error (1SE) envelope, with the exception of a peak around 1300 CE; this peak does not approach the upper 2SE uncertainty interval.

The overall amplitude for the EV's of the two reconstructions is 1.23 °C for decadal changes in D1200 and 0.55 °C for multidecadal changes in NAM480. We compared NAM480 to three high-resolution hemispheric-scale temperature reconstructions (Moberg *et al* 2005, Mann *et al* 2009, Ljungqvist 2010) and one temperature reconstruction for the Arctic region (Kaufman *et al* 2009) that cover the same time span (500–1980 CE for Mann *et al* 2009, 480–1980 CE for the other reconstructions). For this purpose, we reduced the resolution of the original annual (decadal for Kaufman *et al* (2009) and Ljungqvist (2010)) time series to tri-decadal resolution using the same approach that we applied to D1200: annual values were averaged over 10 year periods, smoothed with a 110 year lowess filter, and then every third decade was selected for comparison (figure 5). We found that the overall EV amplitude for tri-decadal changes in NAM480 is lower than the amplitude in the other reconstructions (ranging between 0.66 °C for Ljungqvist (2010) and 0.74 °C for Kaufman *et al* (2009)), but falls within the range of amplitudes reported for annual resolution hemispheric-scale temperature reconstructions over the last millennium (ranging from 0.4 °C in Mann *et al* (1999) to 1 °C in Esper *et al* (2002), see also Esper *et al* (2012)).

The 19th century is the coldest period in both D1200 and NAM480. The warmest period in D1200 is the early 14th century, but it is worth noting that this is the warm peak that falls outside of the 1SE envelope of NAM480 (figure 4). The 9th century is the warmest century of NAM480, closely followed by the 11th century. EV warm peaks in NAM480 and D1200 are slightly warmer than the baseline period (1904–1980), but nevertheless much cooler than North American temperatures during the most recent 30 years and the early 21st century in particular (figure 4), which are outside the estimated upper 2SE range over the entire reconstruction period. A related analysis of WS12 (Wahl and Smerdon (2012), cf SOM) finds that recent (1986–2005) temperatures in temperate western North America are not exceeded by any member of an ensemble of 462 000 bidecadal means for the period 1500–1980 CE (1000 reconstruction ensemble members times 462 sequential 20 year periods between 1500 and 1980), and thus very likely represent the warmest bidecadal average during the past 500 years, conditional on the method of uncertainty ensemble generation. The EV temperature differences between the coldest periods in NAM480 (1845–1875) and D1200 (1810–1849) and the most recent 30 year period (1970–1999) are 0.86 °C and 0.73 °C, respectively; similar and very close, respectively, to the difference of 0.7 °C found by Frank *et al* (2010) in a comparable, ensemble-based analysis of 521 estimates of hemispheric-scale temperature variability over the last millennium (with their coldest period being 1601–30).

Both of our reconstructions show an overall cooling trend over the last millennium until 1900 CE, which is reflected by the negative slopes of linear regressions with rates of $-0.32\,°C\ ka^{-1}$ (D1200; 1200–1900 CE) and $-0.34\,°C\ ka^{-1}$ (NAM480; 1000–1900 CE; cf PAGES2K_consortium 2013).

VISIT THE SCIENTIFIC PUBLICATIONS REPORT ARCHIVE

This millennium-scale cooling trend is possibly related to orbital forcing (Berger and Loutre 1991), and is visible in regional late Holocene temperature reconstructions for all continents except Antarctica (PAGES2K_consortium 2013) but is particularly evident (>0.3 °C ka^{-1}) in temperature reconstructions from high-latitude Northern Hemisphere regions (Kaufman *et al* 2009, Esper *et al* 2012, PAGES2K_consortium 2013). The start date of NAM480 is too recent to capture warmth during the RWP (0–400 CE) and this is likely one of the reasons why the cooling trend in this record is not as strong compared to high-latitude temperature reconstructions over the last two millennia (Esper *et al* 2012).

Before late-19th to early-21st century times, there are three prominent low-frequency periods in our extended reconstruction starting at 480 CE, notably the cooler DAC (about 500–700 CE) and LIA (about 1200–1900 CE), and the warmer MCA (about 750–1100 CE). Cool temperatures during the DAC have been recorded at the hemispheric-scale (figure 5) and were accompanied by falling lake levels in the British Isles (Charman *et al* 2006), dry conditions in various tropical monsoon regions (Gupta *et al* 2003, Wang *et al* 2005, Shanahan *et al* 2009), and by political turmoil and social upheaval over large parts of Europe (Berglund 2003, Buntgen *et al* 2011). Our reconstruction suggests that North American temperatures were also cool during this period (figure 4) and thus supports the global extent of this cold period and a possible link to an explosive, near-equatorial volcanic eruption in 536 CE (Larsen *et al* 2008), though it is unlikely that a single eruption would have been the sole causal factor for the DAC.

Temperatures over temperate North America increase after the 7th century and reach warm peaks around 850 and 1050 CE (figure 4). Peak warmth during the 9th through 11th centuries can be found in the hemispheric-scale reconstructions by Mann *et al* (2009), Ljungqvist (2010) and correspond at a regional scale to intense droughts in the American West, as recorded in tree-ring records from a network of living and dead trees (Cook *et al* 2004) and from tree stumps rooted in present-day Mono Lake, California (Stine 1994). The 11th century warmth in particular is well represented in other large-scale temperature reconstructions (figure 5) and this was also the warmest period on record in an ensemble-based analysis of northern hemisphere temperature variability that did not extend back in time beyond 1000 CE (Frank *et al* 2010). These three warm centuries constitute the core of the MCA in our reconstruction, a period characterized in North America by potential anomalous continental summer ridging in the Midwest (Wahl *et al* 2012) and centennial-scale aridity in the West (Cook *et al* 2004, Woodhouse 2004). Anomalous MCA climate conditions and their impacts on ecosystems in North America have been recorded in an array of lacustrine and terrestrial proxies (Gajewski 1987, see Graham *et al* 2007 for an overview). North American Medieval drought and warmer conditions form the regional expression of a global-scale MCA climate configuration (Seager *et al* 2007, Graham *et al* 2011, Landrum *et al* 2013) that is hypothesized to have involved a feedback mechanism between a La Niña-like state of the tropical Pacific (Cobb *et al* 2003, Mann *et al* 2005, Graham *et al* 2007, Emile-Geay *et al* 2008, Mann *et al* 2009), a prolonged tendency towards positive-phase North Atlantic Oscillation (NAO) phase (Trouet *et al* 2009), and an enhanced Atlantic Meridional Overturning Circulation (AMOC; Knight *et al* 2005, Seager *et al* 2007, Delworth and Greatbatch 2000, Trouet *et al* 2012).

Distinctively cooler conditions are already occurring by the early 13th century, and the final relaxation from this particular ocean–atmosphere state into the LIA occurs in NAM480 roughly around 1350 (figure 4). This latter timing corresponds generally with a climatic shift recorded in a wide variety of North American proxies reflecting hydroclimatic conditions (Hughes and Graumlich 1996, Hughes and Funkhouser 1998, Cook *et al* 2004), wildfire occurrence (Swetnam 1993, Trouet *et al* 2010), and sea surface temperature (Kennett and Kennett 2000) variability. The timing of the MCA–LIA transition in NAM480 also corresponds to a transition period in hemispheric-scale temperature reconstructions (figure 5). Small differences in the transition timing between records may reflect dating uncertainty and decreasing sampling and temporal resolution of individual records. However, the widespread signature of this climatic shift suggests that changes in tropical sea surface temperatures (SSTs) were involved (Seager *et al* 2007, Graham *et al* 2011). Model simulations suggest that this climatic shift between the MCA and LIA could be related to an externally driven change in radiative forcing (Shindell *et al* 2003, Vaquero and Trigo 2012) or may have occurred in combination with internal variability of the ocean–atmosphere system (Goosse *et al* 2012, PAGES2K_consortium 2013).

In this study, the MCA–LIA transition (centered on the 14th century) is the period when our two reconstructions D1200 and NAM480 diverge most: cold temperatures prevail in the pollen-based NAM480 record from 1200 CE onwards, whereas the late 13th and early 14th century is the warmest pre-20th century period of the tree-ring-based D1200 record (figure 4). Divergence between the records is however of limited extent (D1200 generally does not exceed the NAM480 1SE uncertainty bands) and may potentially be explained by the difference in the regions of origin of the two proxy archives (figure 1). The majority of tree-ring records in D1200 originate in the North American West, where long-lived trees are relatively abundant and where pollen records are sparse. Previous studies (Douglass 1929, Stine 1994, Ni *et al* 2002, Woodhouse 2004, Cook *et al* 2007) have demonstrated that the late 13th century was a period of severe drought (implying warm summer temperatures; Wahl *et al* 2012) in the American Southwest. This 'Great Drought' (Douglass 1929) extended across large portions of the western United States (Woodhouse 2004, Cook *et al* 2007), but its signal was likely not dominant in the broader region covered by the pollen records of NAM480. This is an interesting area for further research in North American last two millennia paleoclimatology, and in particular in relation to the joining of pollen-derived and tree ring-derived paleoclimate data.

The common cool period LIA in our reconstructions roughly covers 1350–1900 CE and its cold peak occurs in the

VISIT THE SCIENTIFIC PUBLICATIONS REPORT ARCHIVE

19th century in both records (figure 4). The 19th century is a well-documented cool period on both regional (particularly in Europe and North America; Briffa *et al* 1992, Lamb 1995, Trigo *et al* 2009) and northern hemispheric scales (Jones and Mann (2004); see also figure 5). A combination of anomalously strong volcanic activity (Cole-Dai *et al* 2009, Chenoweth 2001, Crowley 2000), continued orbital cooling (Kaufman *et al* 2009, Esper *et al* 2012), and low solar irradiance (the so-called Dalton minimum; 1790–1830; Lean *et al* 1995, Mann *et al* 1998) likely contributed to this global-scale cooling event (PAGES2K_consortium (2013), cf figures 3 and 4).

In many hemispheric-scale temperature reconstructions (Moberg *et al* 2005, Mann *et al* 2009, Frank *et al* 2010, Ljungqvist 2010), the 19th century cool anomaly is exceeded in amplitude by coldness in the 16th and/or 17th century. Only a few of these reconstructed 16th–17th century temperatures (e.g., Moberg *et al* 2005) fall outside of the 2SE uncertainty range of NAM480 and a comparison between D1200 and other continental-scale temperature reconstructions generates no notable differences for this period (figure 3 in PAGES2K_consortium (2013)). Nevertheless, both NAM480 and D1200 represent generally higher temperatures during the 16th and 17th centuries than the hemispheric-scale and Arctic region reconstructions (figure 5). A possible explanation for relatively high temperatures in North America in this study is the 16th century mega-drought, a remarkably widespread and persistent period of drought in the late 16th century (Woodhouse and Overpeck 1998). Drought conditions during this period, likely associated with warmer than usual summer temperatures, were widespread and their spatial coverage included northern Mexico, British Columbia, and eastern coastal US regions (Stahle *et al* 2000). The atmospheric circulation patterns leading to such widespread yet regional drought and warmth remain to be explored (Woodhouse 2004).

4. Conclusion

A multi-proxy approach, in which tree-ring data were calibrated against instrumental temperature data and in turn used as a calibration target for lower-resolution pollen data, allowed us to develop an annual temperature reconstruction that extends back to 480 CE and spatially covers the majority of temperate North America. Three prominent low-frequency periods (DAC, MCA, LIA) are evident in our reconstruction that are also reflected in other continental (PAGES2K_consortium 2013) to hemispheric-scale temperature reconstructions around the globe. Discrepancies between the two reconstructions (e.g., 13th–14th centuries) and between our reconstructions and other temperature reconstructions (e.g., 16th century) can potentially be explained by the presence of regional-scale droughts. The increased spatial and temporal coverage provided by this multi-proxy reconstruction contributes to our improved understanding of natural climate variability in the context of future anthropogenic impacts on North American climate.

Acknowledgments

This study was conducted in the framework of the Past Global Changes (PAGES) Programme of the International Geosphere Biosphere Programme (IGBP). Support for PAGES activities is provided by the US and Swiss National Science Foundations and by the US National Oceanographic and Atmospheric Administration.

Appendix. WS12 and 1200-on reconstructions—detail and comparison

The figures below show the annual reconstruction values for WS12 (figure A.1) and the 1200-on reconstruction (figure A.2), and comparison of the 1200-on reconstruction to the 95% reconstruction uncertainty range of WS12

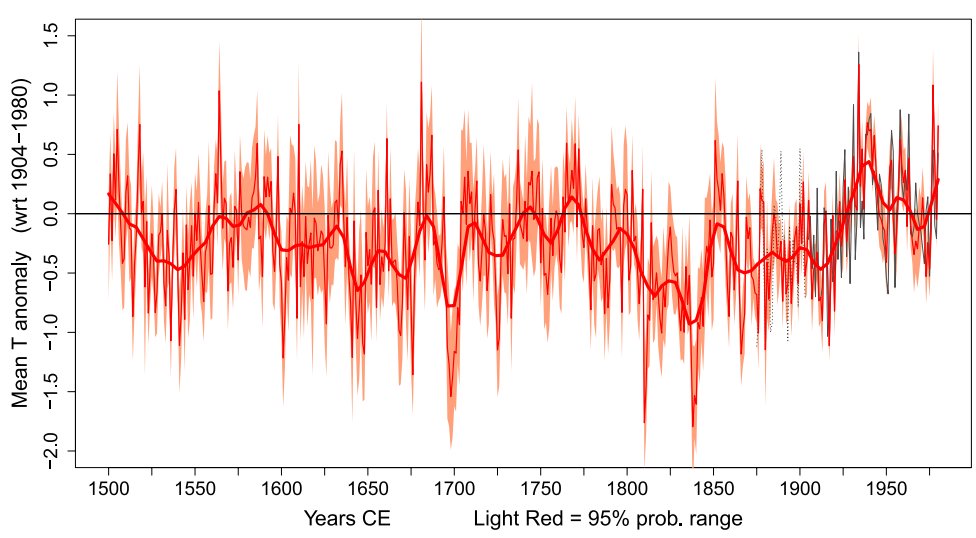

Figure A.1. Temperate North America WS12 reconstruction (30°–55°N by 95°–130°W; 1500–1980).

VISIT THE SCIENTIFIC PUBLICATIONS REPORT ARCHIVE

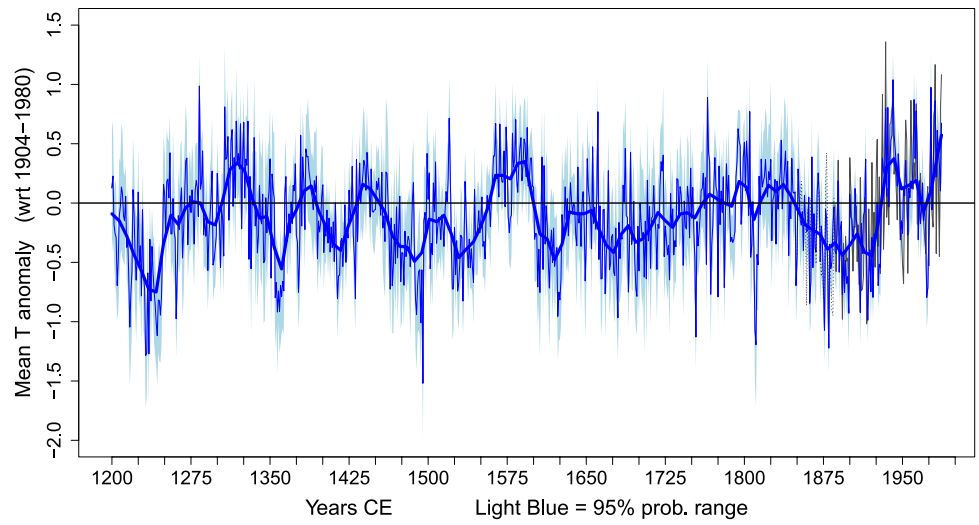

Figure A.2. Temperate North America 1200-on reconstruction (30°–55°N by 95°–130°W; 1200–1980).

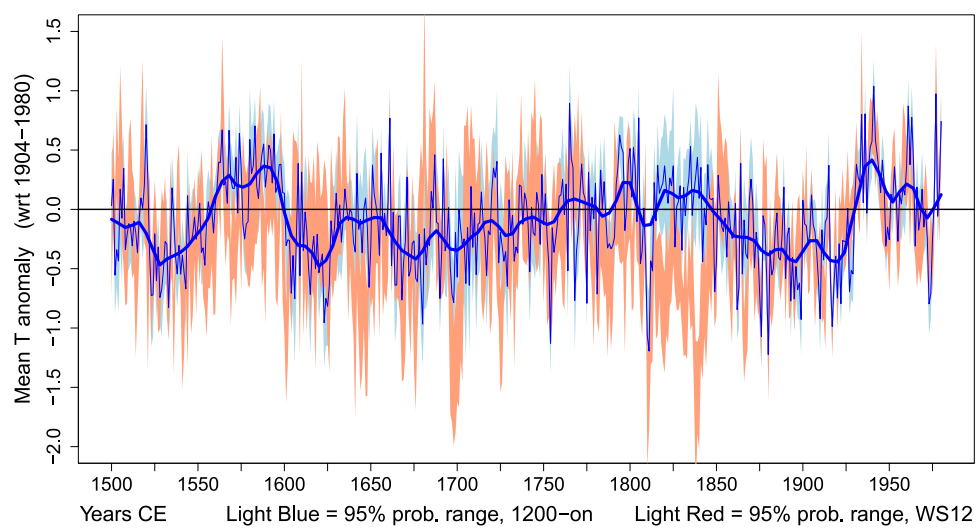

Figure A.3. Temperate North America 1200-on reconstruction (30°–55°N by 95°–130°W; 1500–1980).

during their period of overlap (1500–1980) (figure A.3). All reconstructions are for annual mean surface temperature of the defined region, 30–55°N by 95–130°W.

In each case, the 95% probability ranges estimated for each year from the Monte Carlo bootstrapping methodology used (Wahl and Smerdon 2012) is shown by light shading that corresponds to the primary color of the bootstrap median reconstruction. The heavy lines are an approximately 20 year lowess smooth. The corresponding instrumental data in figures A.1 and A.2 is shown in solid gray (calibration) and dotted gray (validation). The zero reference in each case is 1904–1980 CE.

References

Berger A and Loutre M F 1991 *Quat. Sci. Rev.* **10** 297–317
Berglund B E 2003 *Quat. Int.* **105** 7–12
Bradley R S, Hughes M K and Diaz H F 2003 *Science* **302** 404–5
Briffa K R, Jones P D and Schweingruber F H 1992 *J. Clim.* **5** 735–54
Buntgen U *et al* 2011 *Science* **331** 578–82
Charman D J, Blundell A, Chiverrell R C, Hendon D and Langdon P G 2006 *Quat. Sci. Rev.* **25** 336–50
Chenoweth M 2001 *Geophys. Res. Lett.* **28** 2963–6
Christiansen B and Ljungqvist F C 2012 *Clim. Past* **8** 765–86
Cobb K M, Charles C D, Cheng H and Edwards R L 2003 *Nature* **424** 271–6
Cole-Dai J, Ferris D, Lanciki A, Savarino J, Baroni M and Thiemens M H 2009 *Geophys. Res. Lett.* **36** L22703
Cook E R, Briffa K R and Jones P D 1994 *Int. J. Climatol.* **14** 379–402
Cook E R, Seager R, Cane M A and Stahle D W 2007 *Earth Sci. Rev.* **81** 93–134
Cook E R, Woodhouse C A, Eakin C M, Meko D M and Stahle D W 2004 *Science* **306** 1015–8
Crowley T J 2000 *Science* **289** 270–7
Delworth T L and Greatbatch R J 2000 *J. Clim.* **13** 1481–95
Diaz H F, Trigo R, Hughes M K, Mann M E, Xoplaki E and Barriopedro D 2011 *Bull. Am. Meteorol. Soc.* **92** 1487–500
Douglass A E 1929 *Natl Geogr. Mag.* **56** 736–70
Emile-Geay J, Seager R, Cane M A, Cook E R and Haug G H 2008 *J. Clim.* **21** 3134–48

VISIT THE SCIENTIFIC PUBLICATIONS REPORT ARCHIVE

Esper J, Cook E R and Schweingruber F H 2002 *Science* **295** 2250–3

Esper J *et al* 2012 *Nature Clim. Change* **2** 862–6

Fedorova I T, Volkova Y A and Varlyguin D L 1994 World vegetation cover. Digital raster data on a 30 min Cartesian orthonormal geodetic (lat/long) 1080 × 2160 grid *Global Ecosystems Database Version 2.0* (Boulder, CO: USDOC/NOAA National Geophysical Data Center)

Frank D C, Esper J, Raible C C, Buntgen U, Trouet V, Stocker B and Joos F 2010 *Nature* **463** 527–30

Gajewski K 1987 *Vegetatio* **68** 179–90

Gajewski K 1988 *Quat. Res.* **29** 255–62

Goosse H, Guiot J, Mann M E, Dubinkina S and Sallaz-Damaz Y 2012 *Glob. Planet. Change* **84/85** 35–47

Graham N E, Ammann C M, Fleitmann D, Cobb K M and Luterbacher J 2011 *Clim. Dyn.* **37** 1217–45

Graham N *et al* 2007 *Clim. Change* **83** 241–85

Gupta A K, Anderson D M and Overpeck J T 2003 *Nature* **421** 354–7

Hughes M and Funkhouser G 1998 *The Impacts of Climate Variability on Forests* (*Springer Lecture Notes in Earth Sciences*) ed M Beniston and J Innes (Berlin: Springer) pp 99–107

Hughes M K and Graumlich L 1996 NATO ASI Series I *Glob. Environ. Change* **41** 109–24

IPCC 2007 *Climate Change 2007: The Physical Science Basis. Contribution of Working Group I to the Fourth Assessment Report of the Intergovernmental Panel on Climate Change* (Cambridge: Cambridge University Press)

Jansen E *et al* 2007 *Climate Change 2007: The Physical Science Basis. Contribution of Working Group I to the Fourth Assessment Report of the Intergovernmental Panel on Climate Change* ed S Solomon *et al* (Cambridge: Cambridge University Press)

Jones P D and Mann M E 2004 *Rev. Geophys.* **42** Rg2002

Jones P D *et al* 2009 *Holocene* **19** 3–49

Kaufman D S *et al* 2009 *Science* **325** 1236–9

Kennett D J and Kennett J P 2000 *Am. Antiquity* **65** 379–95

Knight J R, Allan R J, Folland C K, Vellinga M and Mann M E 2005 *Geophys. Res. Lett.* **32** L20708

Lamb H H 1995 *Climate, History and the Modern World* (London: Routledge)

Landrum L *et al* 2013 *J. Clim.* **26** 1085–111

Larsen L B *et al* 2008 *Geophys. Res. Lett.* **35** L04708

Lean J, Beer J and Bradley R 1995 *Geophys. Res. Lett.* **22** 3195–8

Ljungqvist F C 2010 *Geogr. Ann.* A **92A** 339–51

Ljungqvist F C, Krusic P J, Brattstrom G and Sundqvist H S 2012 *Clim. Past* **8** 227–49

Mann M E, Bradley R S and Hughes M K 1998 *Nature* **392** 779–87

Mann M E, Bradley R S and Hughes M K 1999 *Geophys. Res. Lett.* **26** 759–62

Mann M E, Cane M A, Zebiak S E and Clement A 2005 *J. Clim.* **18** 447–56

Mann M E, Zhang Z H, Hughes M K, Bradley R S, Miller S K, Rutherford S and Ni F B 2008 *Proc. Natl Acad. Sci.* **105** 13252–7

Mann M E, Zhang Z H, Rutherford S, Bradley R S, Hughes M K, Shindell D, Ammann C, Faluvegi G and Ni F B 2009 *Science* **326** 1256–60

Moberg A, Sonechkin D M, Holmgren K, Datsenko N M and Karlen W 2005 *Nature* **433** 613–7

Ni F B, Cavazos T, Hughes M K, Comrie A C and Funkhouser G 2002 *Int. J. Climatol.* **22** 1645–62

PAGES2K_consortium 2013 *Nature Geosci.* at press (doi:10.1038/NGEO1797)

Seager R, Graham N, Herweijer C, Gordon A L, Kushnir Y and Cook E 2007 *Quat. Sci. Rev.* **26** 2322–36

Shanahan T M, Overpeck J T, Anchukaitis K J, Beck J W, Cole J E, Dettman D L, Peck J A, Scholz C A and King J W 2009 *Science* **324** 377–80

Shindell D T, Schmidt G A, Miller R L and Mann M E 2003 *J. Clim.* **16** 4094–107

Smith T M, Reynolds R W, Peterson T C and Lawrimore J 2008 *J. Clim.* **21** 2283–96

Stahle D W, Cook E R, Cleaveland M K, Therrell M D, Meko D M, Grissino-Mayer H D, Watson E and Luckman B H 2000 *EOS Trans. AGU* **81** 121–5

Stine S 1994 *Nature* **369** 546–9

Swetnam T W 1993 *Science* **262** 885–9

Trigo R M, Vaquero J M, Alcoforado M J, Barriendos M, Taborda J, Garcia-Herrera R and Luterbacher J 2009 *Int. J. Climatol.* **29** 99–115

Trouet V, Esper J, Graham N E, Baker A, Scourse J D and Frank D C 2009 *Science* **324** 78–80

Trouet V, Scourse J D and Raible C C 2012 *Glob. Plan. Change* **84/85** 48–55

Trouet V, Taylor A H, Wahl E R, Skinner C N and Stephens S L 2010 *Geophys. Res. Lett.* **37** L04702

Vaquero J and Trigo R 2012 *Sol. Phys.* **279** 289–94

Viau A E, Gajewski K, Sawada M C and Fines P 2006 *J. Geophys. Res.: Atmos.* **111** D09102

Viau A E, Ladd M and Gajewski K 2012 *Glob. Planet. Change* **84/85** 75–83

Wahl E R, Diaz H F and Ohlwein C 2012 *Glob. Planet. Change* **84/85** 66–74

Wahl E R and Smerdon J E 2012 *Geophys. Res. Lett.* **39** L06703

Wang Y J *et al* 2005 *Science* **308** 854–7

Wanner H *et al* 2008 *Quat. Sci. Rev.* **27** 1791–828

Woodhouse C A 2004 *Aquat. Sci.* **66** 346–56

Woodhouse C A and Overpeck J T 1998 *Bull. Am. Meteorol. Soc.* **79** 2693–714

VISIT THE SCIENTIFIC PUBLICATIONS REPORT ARCHIVE